



NTNU – Trondheim
Norwegian University of
Science and Technology

Experiments on gas flow with wet pipe walls

Thomas Arnulf

Master of Science in Mechanical Engineering

Submission date: June 2013

Supervisor: Ole Jørgen Nydal, EPT

Co-supervisor: Andrea Shmueli, EPT

Norwegian University of Science and Technology
Department of Energy and Process Engineering

EPT-M-2013-11

MASTER THESIS

For

Stud.techn. Thomas Arnulf

Spring 2013

Experiments on gas flow with wet pipe walls*Forsøk med gass strøm i rør med væskefilm på veggen***Background**

The entrained droplet field in the gas core of separated gas-liquid flows in pipelines affects the flow in two ways: the droplet field provides efficient liquid transport and the droplet can deposit on the wall and enhance the wall friction. Droplet flux measurements are currently being made at the Sintef Multiphase Flow Laboratory in a PhD project. The current master project is directed towards pressure drop in gas flows with wet walls.

An experimental setup will be made to determine the pressure drop in gas flows with small amounts of liquid on the wall. The amount of liquid will be measured by quick closing valves in a vertical section in the Multiphase Flow Laboratory.

The data will be useful for comparisons with predictions from flow simulators.

The following tasks are to be considered:

1 Literature review on gas flow with wet walls

2 Vertical flushing experiments: A liquid filled pipe will be purged with an air stream, until all liquid is removed. At different time intervals, the pipe will be closed with valves, and the holdup measured. This will yield a pressure drop curve vs. holdup for gas flows with wet walls. Experiments can be made with two liquid viscosities.

3 Comparisons with models from the literature, and with available flow simulators (OLGA, LedafLOW)

4 If possible, reporting in the form of a publication

Within 14 days of receiving the written text on the master thesis, the candidate shall submit a research plan for his project to the department.

When the thesis is evaluated, emphasis is put on processing of the results, and that they are presented in tabular and/or graphic form in a clear manner, and that they are analyzed carefully. The thesis should be formulated as a research report with summary both in English and Norwegian, conclusion, literature references, table of contents etc. During the preparation of the text, the candidate should make an effort to produce a well-structured and easily readable report. In order to ease the evaluation of the thesis, it is important that the cross-references are correct. In the making of the report, strong emphasis should be placed on both a thorough discussion of the results and an orderly presentation.

The candidate is requested to initiate and keep close contact with his/her academic supervisor(s) throughout the working period. The candidate must follow the rules and regulations of NTNU as well as passive directions given by the Department of Energy and Process Engineering.

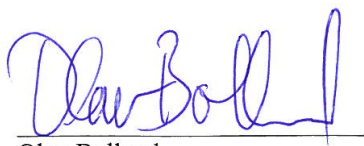
Risk assessment of the candidate's work shall be carried out according to the department's procedures. The risk assessment must be documented and included as part of the final report. Events related to the candidate's work adversely affecting the health, safety or security, must be documented and included as part of the final report.

Pursuant to "Regulations concerning the supplementary provisions to the technology study program/Master of Science" at NTNU §20, the Department reserves the permission to utilize all the results and data for teaching and research purposes as well as in future publications.

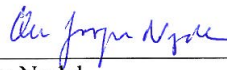
The final report is to be submitted digitally in DAIM. An executive summary of the thesis including title, student's name, supervisor's name, year, department name, and NTNU's logo and name, shall be submitted to the department as a separate pdf file. Based on an agreement with the supervisor, the final report and other material and documents may be given to the supervisor in digital format.

- Work to be done in lab (Multiphase Flow Laboratory)
 Field work

Department of Energy and Process Engineering, 16 January 2013



Olav Bolland
Department Head



Ole Jørgen Nydal
Academic Supervisor

Co-supervisor: Andrea Shmueli (PhD)

Preface

This thesis concludes the work of my master project, at the Department of Energy and Process Engineering at NTNU in the spring of 2013. I would first of all like to thank my supervisor professor Ole Jørgen Nydal for providing me with an interesting project, and for his guidance and advice throughout the semester. I would also like to thank my co-supervisor P.hD student Andrea Shmueli Alvarado for all the help and advice I have received during the work. A huge thank also to all the laboratory people in the department, Paul Svendsen, Martin Bustadmo, Halvor Haukvik, Odin Hoff and Stein Skånøy, who helped out with the experimental setup.

Trondheim, June 10, 2013

Sammendrag

Et nytt forsøksoppsett, bygget for å undersøke muligheten for trykkfallreduksjon i en gasstrømning ved å introdusere en tynn væskefilm på rørveggen er presentert. To forsøksserier er gjennomført, en med vann som væskefilm og en med Nexbase 3080, en olje med høy viskositet. Luft er benyttet som gassfasen i begge seriene. Numeriske simuleringer av forsøk av samme type, tidligere utført ved NTNU, er utført i både OLGa og LedaFlow. I disse forsøkene er vann og oljen Exxsol D80 benyttet som væskefilm, mens gassfasen består av luft. Bergeninger av trykkfall, med forskjellige modeller for friksjonen mellom gass- og væskefasen er også sammenlignet med disse forsøkene.

Forsøkene presentert i denne oppgaven er forbundet med store usikkerheter når det gjelder strømningsraten av gass og målingene av trykkfall. Derfor vil resultatene kun gi indikasjoner på hvordan trykkfallet er avhengig av væskemengden. Det ble ikke observert noen trykkfallreduksjon, sammenlignet med målingene for en-fase gasstrøm. Begge seriene viste at trykkfallet steg som en funksjon av økende væskemengde. Forsøkene ble utført som uttørkningsforsøk, der væskefilmen blir tynnere med tiden. Etter en bestemt tid brøt filmen sammen og rørveggen var til slutt tilnærmet tørr. Denne strømningsutviklingen er dokumentert ved hjelp av bilder fra hvert av tidspunktene hvor målinger ble gjennomført. I tillegg er videoer som viser hele uttørkningsprosessen vedlagt elektronisk i DAIM.

Begge simuleringsprogrammene som ble benyttet overestimerte trykkfallet for gitte verdier for væskemengde, sammenlignet med forsøksdata. Dette ble også observert for de fleste testede friksjonsmodellene. En av modellene passet derimot godt med alle datapunktene i begge forsøksseriene.

Abstract

A new experimental setup, for investigation of a possible pressure drop reduction in gas transport pipelines through introduction of a liquid film at the pipe walls, is presented. Two experimental series are performed, using the high viscosity oil Nexbase 3080 and water as liquid films. Air was used as the gas phase in both series. Numerical simulations of the phenomena are performed in the commercial softwares OLGA and LedaFlow, and the results are compared with the experimental results of similar experiments performed earlier at NTNU. In these experiments the liquid film consisted either of water or Exxsol D80, while air again was used as the gas phase. Pressure drop calculations, taking in different models for the interfacial friction factor in annular flow, was also compared with these experiments.

In the experiments presented, large uncertainties were related to the flow rate of air, and also to the pressure drop measurements. Therefore the results only serves as indications on the behaviour of the pressure drop as a function of holdup. No pressure drop reduction, compared to the single-phase pressure drop, was observed in any of the series. For both liquids, the pressure drop was found to increase whenever small amounts of liquids were present. The experiments were performed as dry-up processes, where the film becomes thinner with time, before it breaks down. This evolution is presented in the form of flow visualizations taken at each of the measurement times. Videos showing the full dry-up processes are attached electronically in DAIM.

Both simulators tested were found to overpredict the pressure drop as a function of holdup. Most of the interfacial friction factor models also overpredicted the pressure drop observed in the experiments they were tested against. One model fitted all the experimental data points well for both water and ExxsolD80.

Contents

1	Introduction	1
2	Objectives	3
3	Literature Review	4
4	Experimental Setup	13
4.1	Setup	13
4.2	Procedure	19
4.3	Experimental conditions	20
5	Experimental Results	26
5.1	Water	26
5.2	Nexbase 3080	32
5.3	Discussion of experimental results	37
6	Simulations	38
6.1	Experimental setup	38
6.2	OLGA simulations	39
6.3	OLGA parametric study	44
6.4	LedaFlow simulations	47
6.5	Discussion of simulation results	51
7	Models for interfacial friction factor	53
8	Conclusion	58
Appendices		
A	PVT file - water	I
B	PVT file - Exxsol D80	III
C	PVT file - Nexbase 3080	V
D	Risikovurderingsrapport	VII
E	Vedlegg til Risikovurderingsrapport	XVIII

1 Introduction

In production from subsea gas fields and exportation of gas, the gas is transported through long pipelines. When gas flows inside a pipe it is exerted to a frictional force, and in the case of upwards inclined pipes an additional gravitational force, which works in the opposite direction of the flow. Because of these forces we can observe a loss of pressure along the pipeline. In order to make the gas flow, a pressure difference being equal to or larger than the total pressure loss in the pipeline is needed. This pressure difference has a direct influence on operational costs of production or transportation of gas. A direct way to cut the costs associated with gas pipelines is therefore to reduce the pressure loss by a reduction of the frictional force working on the gas. If this can be achieved, it will also increase the utilization of gas fields. As there is a natural pressure difference between the reservoir and the production site, a smaller pressure drop will lead to more transported gas before the pressure difference is reduced to the total pressure drop. Also if a larger flowrate is requested a larger pressure difference is required.

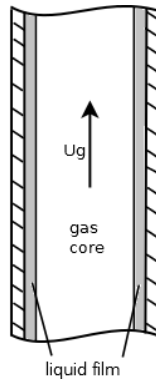


Figure 1: Illustration of annular flow in a vertical pipe

The pressure loss caused by friction is exerted on the gas at the gas-wall interface. Viscosity, density and velocity of the gas, together with wall material and surface roughness, are factors that directly influence the frictional part of the pressure drop. A way to alter this term is to introduce a thin liquid film on the pipe walls. The frictional force will then be dependent on the liquid-gas interface and the liquid-wall interface. A theoretical reduction of pressure drop in this manner is showed in [18], but it is so far not been verified in experiments. In [6] a

section is devoted to the experimental investigation of the possibility of pressure loss reduction by the use of wet walls. No reduction was observed but the author suggests that new experiments should be carried out.

In this thesis a further investigation of a possible reduction of pressure drop in gas pipelines by introduction of a thin liquid film will be the focus.

2 Objectives

- Perform a literature review on gas flows with wet walls
- Perform series of experiments on gas flow with wet walls in a vertical pipe, to obtain the relation curve between liquid holdup and pressure drop. The series differ in the choice of the liquid viscosity.
- Conduct OLGA simulations with the same conditions as in the experimental series
- Conduct series of LedaFlow simulations with the same conditions as in the experimental series
- Compare the experimental results with flow models from the literature
- Compare results from the flow simulators OLGA and LedaFlow with the experimental results
- Present the work in the form of a publication

3 Literature Review

Modelling approaches and experimental work on gas flow in pipes with a thin annular liquid film are the main topics of this section. Other contributions, concerning for instance gas flow over a thin liquid film for other geometries, are included if they are found to improve the understanding of the phenomena in gas flows with wet pipe walls.

The work presented in [18] provides the main motivation for a further investigation of the possibility of pressure drop reduction using a stable liquid film. Two theoretical modelling approaches are made, both solves the velocity profile of the laminar liquid film directly from the Navier-Stokes equation. To solve the velocity profile of the turbulent gas core, the authors first use the law of the wall. This is a direct model taking in viscosity and density of the gas, shear stress at the gas-liquid interface, and the distance from the gas-liquid interface. Secondly the gas velocity profile is solved using the Reynolds-averaged Navier-Stokes equation and the eddy-viscosity assumption. To solve for the eddy viscosity Nikuradse's mixing length model is used. According to the authors both models for the turbulent gas core are experimentally verified for pipe flow. From the known velocity profiles the mass flow rate of gas can be found by integration over the cross section. In the first case this is done analytically, for the second case only a numerical integration was possible. Calculations are made with varying liquid viscosities and film thicknesses. The mass flow rates are in both cases compared to the case with no liquid film at the pipewall. Both cases shows a theoretical possibility of increasing the mass flow rate of gas by introducing a liquid film at the wall. Increasing film thickness were the main parameter found to result in larger mass flow rate, until a certain thickness where the cross sectional area become so small that it would limit the capacity. A low liquid viscosity was also found to give a high mass flow rate of gas. In their conclusion the authors characterize the results as promising and suggests further thorough investigations.

In [6] a section is devoted to an experimental investigation of the results in [18]. Using a setup of a vertical test section, pressure drop and holdup are measured with a decreasing amount of liquid holdup, i.e. decreasing thickness of the liquid film. Two experimental series were performed both using air as the gas phase. For the liquid phase water and oil (Exxsol D80) were used for one series each. In these experiments no pressure drop reduction, compared to single phase gas flow, was found. On the contrary the liquid film increased the pressure drop in both series. The author concludes that the liquid film develops an equivalent sand roughness that scales with the film thickness. It is also mentioned that waves in the film induced by fluctuations in the turbulent gas core probably caused film instabilities. Pressure drop reduction using liquid film was on the other hand calculated assuming a stable liquid film. Similar experiments were conducted

using horizontal test sections of both acrylic and steel pipes. These experiments showed no pressure drop reduction, but rather an increase compared to single-phase flow also here. Reasons for not realizing the potential pressure drop were, according to the author, asymmetric film around the pipe circumference, film breakdown takes place too soon, flow in film is not laminar, gas-liquid interface is not smooth.

To extend the investigations, annular flow models are compared to the experimental series in [6]. Models for both laminar and turbulent liquid films are presented. For the turbulent film approach both smooth and rough interfaces are considered. The laminar film model suggests a pressure drop reduction which is not observed in the experiments. Comparisons of the turbulent film models and the experimental results are not presented.

Another contribution to the experimental investigation of the potential pressure loss reduction shown in [18], is presented in [7]. In order to test the effect of wall wetting and fluid viscosity four different experiments were conducted using combinations of stainless steel pipes, acrylic pipes, oil and water. Air was used as the gas phase. All four series were dry-up experiments where the pressure drop was measured for a gas flow of $Re \sim 10^6$ with decreasing liquid film at the wall. The measured pressure drop in the experiments were then compared to a theoretical computed pressure drop in dry gas pipeflow with equal gas Reynolds number. None of the four tested cases showed a pressure drop falling below the theoretical value for dry gas. The observed behaviour of the pressure drop after closing the liquid supply was an initial drop in the first minutes followed by convergence to the dry pipeflow value. According to the authors gravity could be a factor that is preventing drag reduction by introducing a laminar liquid film in a horizontal pipeflow as the film will not be symmetrical. Also it is pointed out that the dewetting process was too fast as the top wall was free of film after a very short time, together with the observations of the gas-liquid interface being wavy and only becoming smooth when the film was very thin. The last possible cause for not obtaining the theoretical drag reduction mentioned in the report, was that the liquid film may not necessarily have been laminar. To overcome these factors and obtain a drag reducing film the authors suggest new experiments using a vertical pipe setup, a more viscous oil and to add wetting chemicals. When comparing the different experiments in the report it is concluded that the choice of fluid influences the pressure drop. Oil is found to have a better chance of creating a drag reducing film as it is dewetting slower and is more viscous than water, and therefore a smooth laminar film is more easily obtained.

In [9] general flow behaviour in three-phase flow with liquid loadings less than 1% is studied experimentally. This technical report provides information on how the pressure drop and holdup are influenced by gas and liquid flow rates, pipe inclination and test section material. Series are conducted using air, water and

oil (Exxsol D80), in horizontal and inclined pipes of steel and acrylic, with gas Reynolds number varying from 10^3 to $2 \cdot 10^5$. An important observation made in these experiments is that the pressure drop increases sharply when small amounts of liquids are present in the flow, compared to single phase gas flow. The pressure drop was also found to be lower in the steel pipe than in the acrylic pipe, and also found to increase non-linearly with increasing superficial gas velocity. With a rather high gas flow rate and low liquid loading the flow is found to be friction dominated i.e. the pressure drop is little affected by the pipe inclination. The liquid holdup is found to be only slightly influenced by the pipe material and choice of fluid. Generally the liquid holdup was found to be a bit larger in the steel pipe than in the acrylic one.

A study of the relative contributions to the total pressure drop is presented in [8]. An equation for the pressure drop is obtained using a two-fluid model, taking the averaged one-dimensional momentum conservation equation for both the gas and the liquid phase and solve for the pressure gradient term. Based on the same equations one can also obtain a liquid holdup equation by canceling out the pressure gradient terms. To be able to solve for all the unknowns, Hålands friction factor correlation for turbulent flows was used to calculate the gas-wall friction. The two other equations then gave the liquid-wall friction and the interfacial friction. In addition the gravitational terms for both phases were calculated using fluid properties, measured holdup and pipe inclination. Stratified flow was assumed in all the calculations in this report. Different experimental data, including both atmospheric and high pressure experiments, and a simulation series obtained in OLGA were then analyzed by the means of these equations. Total pressure drop and holdup were measured in the experiments. The relative contributions to the total pressure drop from each of the terms were then compared to each other for different configurations. For this thesis, only data from frictional dominated flows with low liquid loading (less than 1%) are found to be relevant. The study revealed that as the liquid loading became smaller the contribution from gas-wall friction became more and more dominant. However liquid-wall friction was found to be dominant in some cases at liquid loadings as low as 0.01%. Pipe diameter and liquid viscosity were found to be factors influencing how small the liquid loading needed to be, for gas-wall friction to contribute more to the total pressure drop than the liquid-wall friction. Small pipe diameter results in a larger wetted perimeter, which according to the authors, together with higher liquid viscosity, will increase the liquid contribution to the pressure drop. As the amount of liquid in the pipes decreases and becomes low enough, the interfacial drag exerted on the gas decreases rapidly.

A modeling approach to gas flows with low liquid contents is presented in [4]. The model is based on transitions from homogeneous flow to stratified flow with curved interface to stratified flow with flat interface, depending on the liq-

liquid holdup. Existing experimental data and observations from horizontal pipes are used to establish the transition points. For this thesis the modeling of the stratified cases are found to be the most relevant, especially with curved interface as this can be compared to vertical annular flow if the film is assumed to cover the whole perimeter. The models pressure drop equation is found by using a modified set of Taitel-Dukler equations, and further assuming a uniform pressure in the cross section. This equation is here presented for annular vertical upflow (1). To find the expression for the interfacial friction factor a statistical analysis was performed to see how it was correlated to the liquid Reynolds number, the gas Reynolds number, the liquid holdup and the film thickness. An expression including all four parameters was found to fit the experimental data in the best way. This interfacial friction expression (2) is, according to the author, the key component of the presented model. To verify this interfacial friction factor, a comparison to existing friction factor correlations is presented. The prediction error of this new correlation are generally much lower than for the others, when comparing with independent data sets. Reasons for the improved results can be that existing correlations also considers much higher holdups and that they assume a flat interface between gas and liquid, while most observations display curved interfaces. Also in this presentation, the pressure drop is found to be higher when a small amount of liquid is present in the gas flow compared to a dry gas stream.

$$A_C \frac{dp}{dx} = g\rho_m - \frac{1}{2}f_i\rho_G(U_{SG} - U_{SL})^2 P_C \quad (1)$$

$$f_i = 303 (Re_L^{0.37} H^{0.34} Re_G^{-0.97} h^{0.31}) + 0.0077 \quad (2)$$

In the calculations showing a potential pressure drop reduction in [18], the liquid film is assumed to be smooth. It is therefore found highly relevant to look into how the interface of a liquid film reacts to fully turbulent gas flows. This has been studied for a long time and an early contribution on the field is presented in [14]. Experiments were conducted using a turbulent air stream over a water film in a horizontal, rectangular channel. Investigated parameters were gas and liquid Reynolds numbers and film height. The gas Reynolds number was found to strongly influence the interface. For the lowest gas flow rates the interface was kept smooth, but as the flow rate increased two-dimensional waves were formed, and as the flow rate was increased even further, different types of three-dimensional waves were observed. For very high gas Reynolds numbers the liquid ended up being dispersed in the gas phase. The onset of two-dimensional waves was found to be in the same gas Reynolds number range as the onset of

turbulence in the gas phase. However stable films was observed for fully turbulent gas flows, and waves sometimes also occurred before the onset of turbulence. This indicates that also flow parameters in the film, e.g. viscosity and film height, are important for the shape of the interface. When investigating the influence of the film height, the authors observed that when the film height was reduced, the film got more stable. The influence of the liquid surface on the gas flow was investigated through the means of velocity profile measurements. The shape of the interface was found to be capable of distorting the velocity profile as the interfacial shear stress became larger for larger waves.

Further investigations on the stability of liquid films sheared by a turbulent gas stream are presented in [11]. Phenomena shown by earlier experiments are explained, new experiments of cocurrent horizontal flow using air and water, with thinner liquid films than in the earlier experiments, were made and theoretical stability analysis using the Orr-Sommerfeld equation is presented in this paper. Thin liquid films were in [14] observed to be more stable than thicker films. The liquid Reynolds number becomes smaller and the internal damping larger, consequently the dynamic instabilities appearing in thicker films are less probable to appear in thin films. It is therefore promising to study thin liquid films when it comes to the possibility of pressure drop reducing films. However as the film thickness was reduced in the experiments presented, a new type of waves was observed. These were non-periodic, slow moving waves occurring for all gas Reynolds number, provided a small enough film height. Other features of these slow waves were steep fronts and long rear portions and the possibility of becoming several times larger than the average film height. The reason for this instability in the thin films is asserted to the tangential stress component on the interface. After the result of this experiments it is concluded that there exist a non-zero film height at which liquid films are most stable. Also the influence of turbulent fluctuations on the stability of the film is discussed. Interestingly enough, the mean air flow profile are found to be the main contributor to instabilities. The reason for this being that the gas fluctuations convected on the film has velocities being much larger than the natural wave velocities in liquid films, resulting in only a weak response of the surface.

The effect of a wavy film interface on the gas velocity profile was studied in [10]. Again experiments were carried out in a horizontal channel with cocurrent flow of air and water. It was found that the drag from a wavy gas-liquid interface were greater than for a dry gas flow with equivalent sand roughness. A theoretical explanation is provided in the paper, saying that for a gas-liquid interface there is a direct exchange of mechanical energy between the phases. By investigating the approximate form of the turbulent energy equation given by Laufer (1951), it is shown that there is net energy transfer from the gas to the liquid for a wavy interface.

Several researchers have also studied the gas-liquid interface in annular flows. This is the case in [16], where experimental studies on the breakdown of the liquid film is presented. A vertical pipe flow around atmospheric pressures is investigated using air, at high flowrates, and water, at low flowrates. No spontaneous breakdown of the liquid film was observed. However if an external disturbance was present, like a dry patch on the pipe wall, then the film would break down, unless the flowrate of the liquid film was sufficient to re-wet the dry patch. Another conclusion made by the authors was that the liquid flow rate needed to prevent breakdown when a disturbance was present, decreased as the gas flow rate increased. If no disturbance was present the film existed in a so called metastable state even for liquid flowrates below the critical value needed for re-wetting.

In the literature on waves in annular two-phase flow in vertical pipes two different types of waves are observed, depending on the liquid Reynolds number. For high values of Re_L so called disturbance waves are observed. These waves are characterized by large spacings between the successive waves and large wave velocities. For lower values of Re_L , long crested, slow moving waves with steep fronts are observed. For this thesis the latter wavetype seems to be the most relevant as they are found in very thin liquid films and also found to have the largest influence on the interfacial shear stress. Together with the observations mentioned above, a theoretical stability analysis, based on the linear momentum equations for each of the phases, to reveal the mechanisms creating these waves are presented in [2]. The work was then compared to experimental data. Two-dimensional unstable disturbances on the liquid film was found to evolve into three-dimensional waves as energy is transferred from the gas to the liquid by nonlinear wave induced gas phase shear stress variations. The ripple waves was also found to have twice the wavelength of the initial disturbance. It is then concluded that the difference in the measured and the predicted wavelengths is due to the predicted waves being two-dimensional, while the ripples are three-dimensional.

Another investigation of waves in annular flow in vertical pipes is presented in [5]. It is here argued that large amplitude roll waves are the main contributor to the extra drag observed in gas flow over liquid films. Experiments were conducted in a vertical pipe being 12 metres long and having a diameter of 0.05 metres. Air and water was used as fluids. Observations showed that the roll waves occurred only if the liquid Reynolds number was above a certain threshold value. The experimental data obtained was then subjected to a statistical analysis enabling the extraction of only the large coherent roll waves from the time series of the film thickness. After this analysis several conclusions about the roll waves were drawn. The roll waves was found to have a random spatial distribution, resulting from a cascade of random interactions during the wave formation. It was also found that the wavelengths was close to the pipe diameter for all values of U_{SL}

and U_{SG} . The height of the waves was also broadly distributed.

There exists many of studies of stability of liquid films and the wave structures occurring on them. The understanding of this field is seems like the biggest challenge, when it comes to reducing pressure drop in gas flows by the introduction of a liquid film. Even though different researchers argue that different waves are the main contributor to the increase of pressure drop in wet flows compared to dry flows, there is a broad agreement that the waves are three-dimensional. A general solution to the stability of liquid films are therefore not found. The papers reviewed also indicates that a stable film sheared by a turbulent gas flow is difficult to obtain. A reduction of pressure drop by introducing a liquid film in a gas flow, as suggested in [18], has not been verified by experiments in any of the reviewed papers. On the contrary, all experimental investigations reported show an increase in pressure drop when a liquid film is present.

In the last part of this chapter different models for the interfacial friction factor in annular flows, found in the literature, are presented. A little introduction to each of them are also given, in order to give an overview of the different backgrounds of the models.

One of the most known models for the interfacial friction factor in annular flows (3) was presented in [19]. The correlation was formed by treating the liquid film as a type of wall roughness, and is similar in its form as wall friction factors using sand grain roughness height . Four sets of annular flow data were used, and the only input parameter is the ratio between the mean film thickness and the hydraulic diameter.

$$f_i = 0.005 \left(1 + 300 \frac{h}{D} \right) \quad (3)$$

In [13] a correlation for the interfacial friction factor based on the observations from [2] is presented, (4). The assumption is that the extra drag exerted on the gas by introduction of a liquid film is the ripple waves that, according to the author, always is present on arbitrary thin films. Density, viscosity and friction velocity for the gas phase are input parameters together with the mean film thickness and the friction factor for a smooth surface.

$$\frac{f_i}{f_s} - 1 = 0.045 \left(\frac{h \rho_G v_G}{\mu_G} - 4 \right) \quad (4)$$

In order to obtain an interfacial friction factor being dependent on relative roughness height and gas Reynolds number, where the dependence on $\frac{h}{D}$ increases as Re_G decreases, (5) was proposed in [12]. The motivation behind this new correlation was the idea that transition roughness causes the interfacial friction factor to depart from the Wallis correlation. Also the old correlations described

by the author did not fit data on thicker films. The Reynolds number used in this correlation is shown in (6).

$$f_i = 0.005 \left\{ 1 + 300 \left[\left(1 + \frac{17500}{Re_G} \right) \frac{h}{D} - 0.0015 \right] \right\} \quad (5)$$

$$Re_G = \frac{\rho_G U_{SG} \left(4 \frac{Ac}{Pc} \right)}{\mu_G} \quad (6)$$

The term 0.0015 in (5) is introduced as a simple shift in the Wallis friction factor, (3), in order to fit the data better for thinner films. The Wallis model with a shift then represents a model of interfacial friction factor in annular flows by itself, and is presented here as (7)

$$f_i = 0.005 \left[1 + 300 \left(\frac{h}{D} - 0.0015 \right) \right] \quad (7)$$

A model for the friction factor based on a flow parameter being similar to the Martinelli parameter was presented in [15]. The correlation is on an iterative form, and can be written as in (8).

$$f_i = f_s \left(1 + 212 \sqrt{\frac{f_i}{f_s} \frac{h}{D}} \right) \quad (8)$$

Another iterative model,(9), was presented in [3]. It is fitted to experiments conducted with relative thin films and is based on the idea that the interfacial friction will increase, compared to dry gas flow, only for liquid films being thicker than the laminar sublayer. The model is presented here in the way it has been rewritten in [12]

$$f_i = f_s \left(1 + 0.45 Re_G^{-0.2} \left(Re_G \sqrt{\frac{f_i}{f_s} \frac{h}{D}} - 4 \right) \right) \quad (9)$$

In [5] a model using a linear relation between mean film thickness and interfacial friction, as in the Wallis correlation, is proposed, (10). The idea behind this linear dependence is based on a sand grain roughness equivalence. It is found that this sand grain roughness of the liquid film is only a function of the standard deviation of the mean film thickness, which in turn is linearly dependent of h . Therefore it is argued that the interfacial friction is only a function of the mean film thickness, and the relation was found to be linear. It must be noted that this model is only valid in the fully rough regime of the interface. Also this friction factor is defined by equation (11), which is different from the Fanning

friction factor definition. The velocity used in this definition is the difference between the bulk velocity and the velocity of the roll waves on the interface. Due to prediction difficulties associated with this roll wave velocity, this model is not compared with experimental results in section 7.

$$f_i = 1.158 \frac{h}{D} + 3.413 \cdot 10^{-4} \quad (10)$$

$$f_i = \frac{\tau_i}{\rho_G (U_B - C_W)^2} \quad (11)$$

4 Experimental Setup

4.1 Setup

In order to conduct a further investigation of the effect of wet walls on pressure drop in gas flows, an experimental setup was built in the Multiphase laboratory located in the department of Energy and Process Engineering at NTNU. The overall configuration is shown in Figure 2, and its components are listed in Table 1.

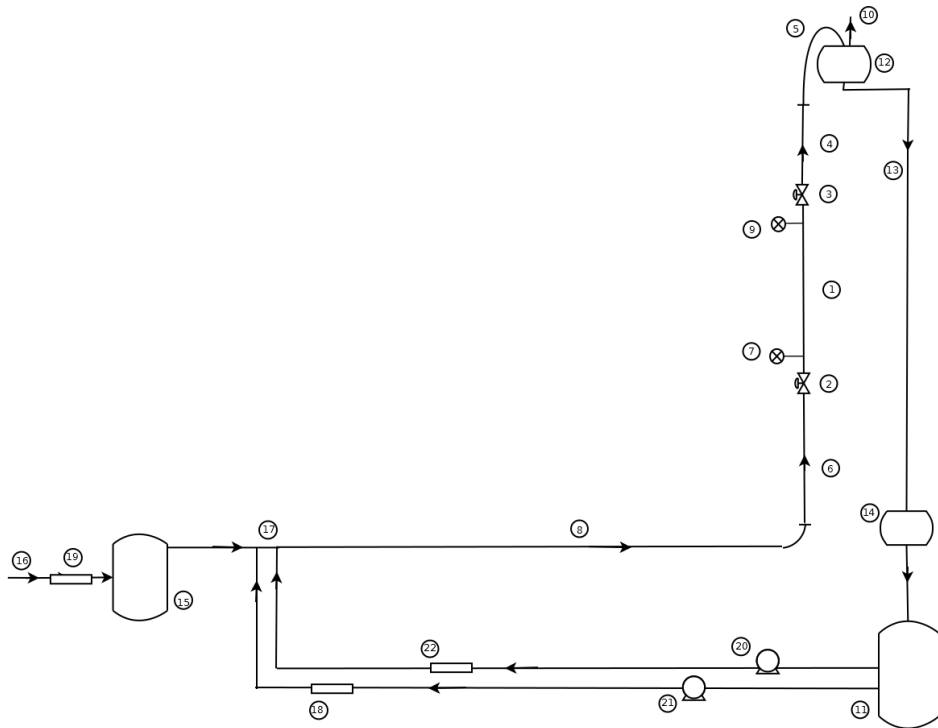


Figure 2: The experimental setup

Air was used as the gas phase in the two-phase flow, while the liquid film consisted either of oil (Nexbase 3080) or water in the experiments. Oil and water are stored together in a large separator in the basement of the laboratory. Small centrifugal pumps were used to transport liquids into the system. Air was to be supplied, with constant mass flow rate, from the workshop air supply at 7 bar.

The air pressure is reduced to 4 bar through a reduction valve.

Figure 2 ID	Component
1	Test section (steel pipe)
2	Quick closing valve
3	Quick closing valve
4	Acrylic pipe section
5	Flexible pipe
6	Steel pipe
7	Pressure transducer
8	Flexible pipe
9	Pressure transducer
10	Air outlet to surroundings
11	Large separator
12	Overflow tank
13	Downflow pipe
14	Buffer tank
15	Air tank
16	Inlet of air, from main air system
17	System inlet (air, oil)
18	Mass flow meter (water)
19	Mass flow meter (air)
20	Centrifugal pump (oil)
21	Centrifugal pump (water)
22	Mass flow meter (oil)

Table 1: Components in experimental setup

After entering through point 17 in Figure 2, the fluids flow through a flexible acrylic pipe before entering the vertical section of the system. The length of this first steel pipe of the vertical section is the length the flow is given to be fully developed. In [20] this development length is given for a turbulent flow by (12). During these experiments the gas Reynolds number, estimated as described in Section 4.3, corresponds to development length in the range of 1.52 m to 1.94 m , while the length of the steel pipe is 2 m

$$\frac{Le}{D} \approx 4.4Re^{\frac{1}{6}} \quad (12)$$

The fluids then flow through the steel test section and a small acrylic pipe section, from which visualization of the flow could be obtained. Both before and after the test section quick closing valves were located, each adding a small pipe element to the setup. After the acrylic pipe the fluids were guided through a flexible pipe and into the top of the overflow tank. From this tank, located 7.35 metre above the horizontal pipe, the liquids was led back to the large separator, via a buffer tank. An opening in the top of the overflow tank made the air flow out to the surroundings and kept the pressure in the tank at 1 atm. The geometry of the setup is summarized in Table 2.

Pipe	L[m]	D [m]	θ [$^{\circ}$]	Figure 2 ID
1 Downwards section	3.77	0.05	-7/-22	8
2 Horizontal section	10.06	0.05	0	8
3 Bend	0.69	0.05	-	8
4 Development section	2.00	0.06	90	6
5 Valve section	0.29	0.06/-	90	2
6 Test section	2.50	0.06	90	1
7 Valve section	0.29	0.06/-	90	3
8 Acrylic pipe section	0.50	0.06	90	4
9 Flexible pipe (outlet)	1.91	0.06	-	5

Table 2: Geometry of setup

In order to accurately measure the holdup at different instants, quick closing valves are installed at both ends of the steel test section. The test section can then be disconnected from the rest of the setup. By opening the bottom valve, the liquid can then be collected in a container. To make sure as much as possible of the liquid is collected a pigging device is created to scrape the remaining liquid of the pipe walls. Accurate holdup measurements can now be extracted by weighting the container on a precision weight. After use of the pigging device the amount of liquid left in the pipe is so small that it can be neglected. As marked in Table 2, the inner diameter of part of the valve sections was a bit larger than the test section diameter. Although this diameter difference can have a small influence on the measured holdup, the liquid film is assumed to be uniform over the lower valve section and in the test section. Following this assumption the measured holdup has been corrected, by subtracting the weight of the liquid corresponding to the film in the valve section.

Accurate determination of the oil density was important in order to measure

holdup accurately on a weight. This was done by filling up a calibrated volume with the oil and then weighting this known volume. The density can now be found by (14). Properties of air, water and oil are listed in Table 3 for 1 atm and 20 °C, which is equal to the experimental conditions. The viscosity of Nexbase 3080 was calculated using a relation developed by SINTEF, equation (13), while the surface tension was found in [17]. Properties of air and water are obtained from [1].

$$\mu[\text{Pas}] = 0.30477e^{-0.054T[^\circ\text{C}]}e^{-0.002096414576171P[\text{bara}]} \quad (13)$$

$$\rho = \frac{m}{V} \quad (14)$$

Fluid	μ [kg/ms]	ρ [kg/m ³]	$\sigma_{g/l}$ [N/m]
Air	$1.9152 \cdot 10^{-5}$	1.204	-
Nexbase 3080	0.1033	833	0.0207
Water	$1.002 \cdot 10^{-3}$	998	0.0728

Table 3: Fluid properties at 20 °C and 1 atm

A Labview program was used to control the different components. The flow of fluids was controlled by the opening percentage of their respective valve. When closing the valves on each side of the test section, the air supply was closed 500 ms in advance, in order to avoid an upstream pressure bulid-up. The quick closing valves could also be opened and closed individually. Pressure drop could be read out in the program from measurements of two absolute pressure transducers, which measurement points had a distance of 1.65 m between them. Specifications

for all the components used in the experiments are listed in Table 4.

Description	Range	Calculated range	Fig 2 ID
Air mass flow meter	4 - 20 mA	0 - 110 l/s	19
Oil mass flow meter	4 - 20 mA	0 - 0.2777 kg/s	22
Water mass flow meter	4 - 20 mA	0 - 0.98172 l/s	23
Centrifugal pump (oil)	0 - 20 mA	0 - 100 % / 0 -50 Hz	20
Centrifugal pump water	0 - 20 mA	0 - 100 % / 0 -50 Hz	21
Quick closing valves	-	-	2, 3
Pressure transducer	1.4 bar	-	9
Pressure transducer	2 bar	-	9

Table 4: Components

To make sure the rig was in accordance with the HSE rules of the department of Energy and Process Engineering at NTNU, a risk assessment was performed. This documentation is included in appendices D and E.

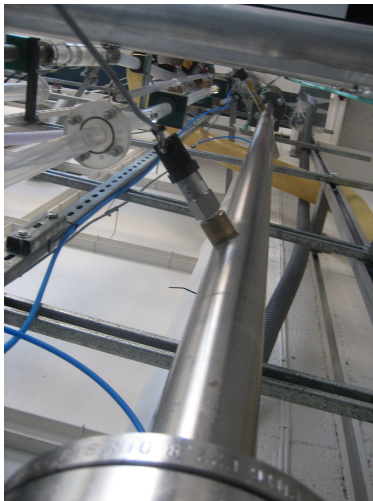


Figure 3: Vertical test section



Figure 4: Quick closing valve



Figure 5: Pressure transducer

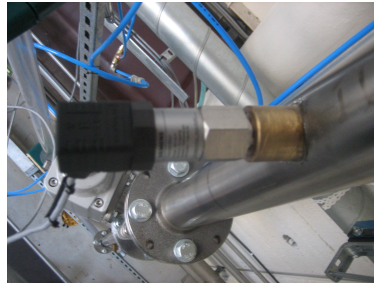


Figure 6: Pressure transducer



Figure 7: Pig for draining the test section



Figure 8: Acrylic pipe for flow visualization



Figure 9: Overflow tank

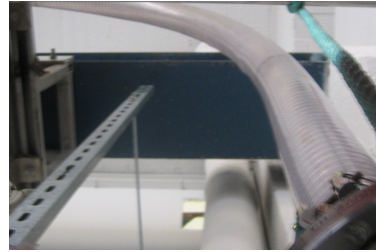


Figure 10: Flexible pipe to overflow tank



Figure 11: Horizontal section



Figure 12: Bend section

4.2 Procedure

Before running any experiments a standardized procedure for running the multi-phase rig in the laboratory was followed. This procedure involves a checklist for physical inspection of all the valves and connections regarding the specific loops used. After this inspection LabView was used for control of the components.

By evaluation of initial tests, the procedure for the water experiments were somewhat different from the procedure of the oil cases. When having water as a liquid film, air and water was introduced together, creating a steady two-phase flow. This flow was kept running for 10 minutes to make sure that steady state

conditions were reached. Then the dry-up process was initiated by shutting off the liquid supply. At prescribed times the quick closing valves was closed to measure the liquid holdup. Pressure drop at this point was read out of logging files in LabView. The liquid content was then emptied from the test section into a small container and weighted. The procedure for the oil experiments was different in the way that no steady two-phase flow was present at the start of the dry-up process. Small amounts of oil was introduced into the horizontal section by setting the oil valve opening to 18% and closing it again after 30 seconds. Then the dry-up process was started by gradually increasing the mass flow of air. Time was measured from the instant at which the desired air flow rate was reached. Again the quick closing valves were closed at desired instants of time, and holdup and pressure drop was measured in the same manner as in the water experiments. As the dry-up of Nexbase 3080 was much slower than for water, and considering the small amount of liquid needed to create a liquid film, it was not found reasonable to start from a stable two-phase flow.

For oil experiments, where holdup was measured after short times, the liquid content in the system could be fairly large at the beginning of the next run. To avoid this and keep good repeatability of the experimental conditions, the dry-up process was continued, after measuring the holdup, so that it in total always lasted for at least 15 minutes before the experimental procedure was repeated.

4.3 Experimental conditions

Several tests were made in order to find appropriate experimental conditions. When using water as the liquid film the experimental conditions were found by testing different valve openings in the gas and liquid supply, in the steady two-phase flow, against each other. The flow in each test was observed visually in the acrylic pipe section. From these tests a flow map was created and is presented in Figure 13. By choosing a gas valve opening of 39% and a liquid valve opening of 20 %, a thin liquid film was created which seemed to have the smoothest interface, and was therefore chosen as experimental conditions. In the case of oil as the liquid film tests were done by introducing oil at the specified valve opening (18%) for different amounts of time, and then observe the dry-up process visually in the acrylic pipe section. The gas valve opening was kept the same as in the water case. By keeping the oil valve open for 30 seconds, a nice film was created within 2 minutes after reaching a constant flow rate of air. This small amount of liquid was chosen for the experiments since it resulted in a dry-up process which was not too long. As Nexbase 3080 is a high viscosity oil, the dry-up time was a factor that had to be accounted for when choosing the experimental conditions.

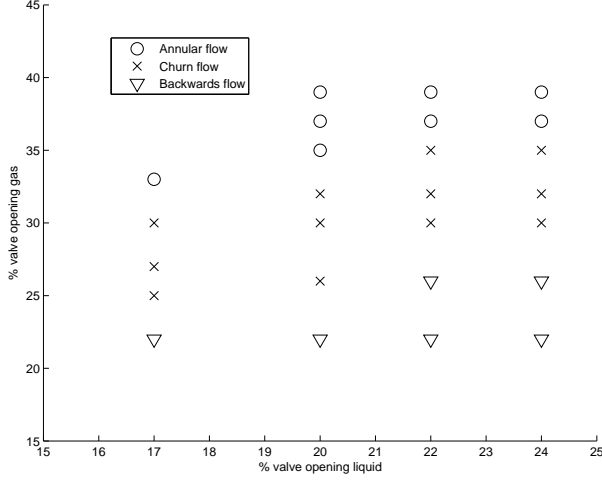


Figure 13: Flow map, air-water

During the testing and running of the setup, problems occurred that have influenced the determination of experimental conditions. The setup was originally installed with a differential pressure transducer, with a range of ± 1 kPa, which had an acceptable error range of about a few percentage of the total range. Under some initial tests using one-phase gas flow, this transducer did not return consistent results, and was discovered to be broken. Two absolute pressure transducers with 1.4 bar and 2.0 bar as specified ranges were therefore installed to enable the execution of any experiments. With the specified ranges of the transducers and an error range of about a few percentage of the total range, it is evident that the errors associated with these transducers are larger than desired when accurate measurements are to be made. However due to time restraints it was decided to run experimental series using the absolute pressure transducers, since they provided consistent measurements for different valve openings of the air supply.

Another problem encountered was associated with the measurements of air flow rates. In a single-phase gas test the measured pressure drop would result in a superficial gas velocity of $U_{SG} = 41.1$ m/s, while the measurements read out in LabView gave $U_{SG} = 9.6$ m/s. Equation (15) are used together with the Darcy friction factor of Blasius for turbulent flows, given in equation (16), to calculate U_{SG} from the pressure drop. The superficial velocity is here specified to be at the outlet so that atmospheric conditions apply. Downstream from the vertical pipe section, the fluids were guided inside a flexible pipe and into the overflow tank, through a bend visualized in Figure 12. This bend is associated with an additional pressure drop contribution which is unwanted when trying to

draw a conclusion on the value of the superficial gas velocity. So in order to make the pressure drop measurements representative for calculation of superficial gas velocities at atmospheric pressure, the single phase measurements are here made after removing the bend from the configuration.

$$-\frac{dP}{dx} = \frac{\lambda_s}{8} \rho_G U_G^2 \frac{S}{A} + \rho_G g \quad (15)$$

$$\lambda_s = \frac{0.184}{Re_k^{0.2}} \quad (16)$$

Values for the air flowrate that is read out in LabView, are measured by a vortex flow meter located on the high pressure side of the rig. A pressure transducer is located next to the flow meter so that the measured flow rates can be pressure corrected and values for flow rates at atmospheric pressure displayed. It was suspected that the discrepancies between the displayed flow rates and the pressure drop measured in the test section were possibly caused by not applying this pressure correction. In order to test this hypothesis the measured flow rates are corrected for pressure, using equation (17) to see if it results in a superficial gas velocity matching the values calculated from the pressure drop measured at atmospheric pressure.

$$U_{SG,atm} = \frac{1}{A} \dot{V}_{meas} \frac{P_{meas}}{P_{atm}} \quad (17)$$

Subjecting the measured volumetric flow rates to this pressure correction gave a corresponding mean superficial gas velocity of 33.1 m/s

No further tests to determine the gas velocity was possible in the time scope of this thesis, and large uncertainties are therefore associated with the experimental results presented in section 5. It has not been possible to establish if the errors results from the pressure measurements or the gas flow meter. Another possibility, which has not been tested at this point is that the flow through the valve sections are introducing the extra pressure drop measured. This last possibility is though not seen as probable, since the extra pressure drop measured is quite large, as seen from the U_{SG} calculated from the measured pressure drop. Figure 14, Figure 15 and Figure 16 shows time series of the three possible superficial gas velocities, and indicates their respective mean values, while the mean values and

the corresponding standard deviations are listed in Table 5. Mean values and standard deviations are calculated from equation (18) and (19) respectively.

Method	\bar{U}_{SG} [m/s]	$\sigma_{U_{SG}}$
Flowrates in LabView	9.6	0.009
Pressure corrected flowrates	33.1	0.047
Pressure drop measurements	41.1	1.075

Table 5: Possible superficial gas velocities

$$\bar{x} = \frac{1}{n} \sum_{i=1}^n x_i \quad (18)$$

$$\sigma_x = \left(\frac{1}{n-1} \sum_{i=1}^n (x_i - \bar{x})^2 \right)^{\frac{1}{2}} \quad (19)$$

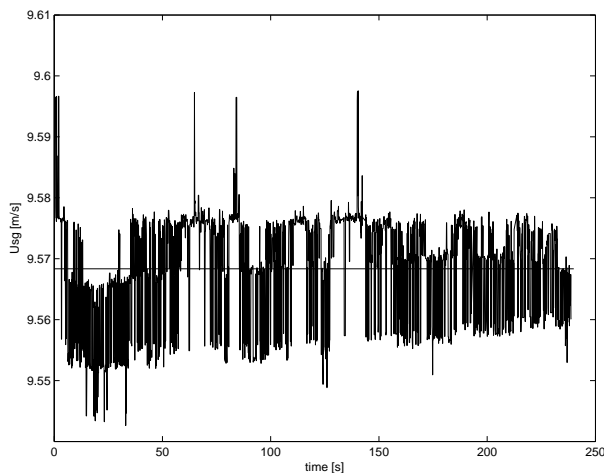


Figure 14: U_{SG} vs time - flowrates in LabView

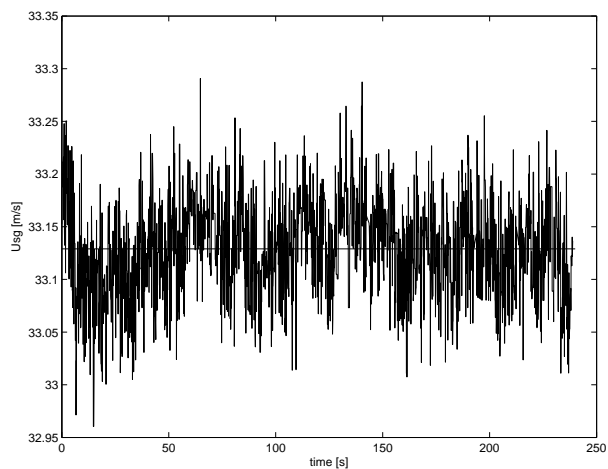
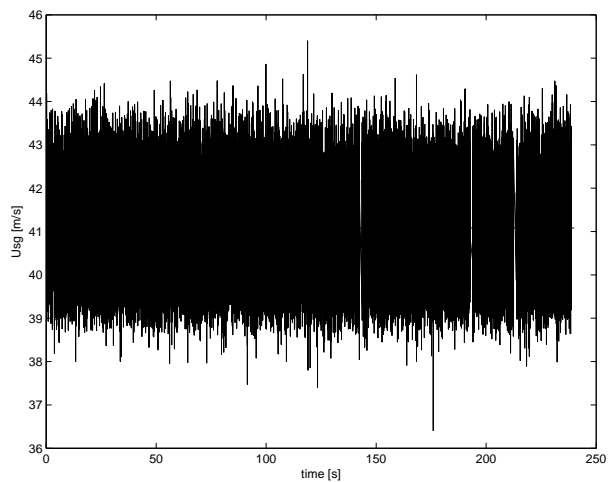
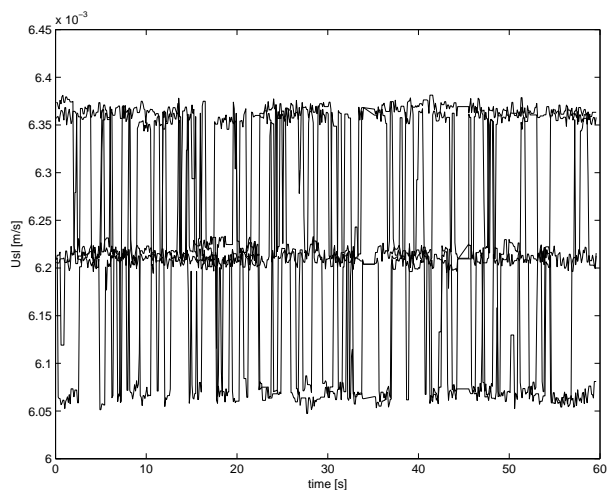
Figure 15: U_{SG} vs time - pressure corrected flowratesFigure 16: U_{SG} vs time - from pressure drop measurements

Figure 17 shows superimposed time series of the superficial liquid velocity of the initial flow in the experiments, with water as the liquid film. 0.0062 m/s was found to be the mean value of the superficial liquid velocity, and the corresponding standard deviation showed to be $\sigma_{U_{SL}} = 1.043 \cdot 10^{-4}$.

Figure 17: Superimposed timeseries of U_{SL} - water

By observing how the pressure drop developed with time and visually observing the liquid film in the acrylic pipe section, measuring times was decided. The measuring times for both series are presented in Table 6.

Liquid film	times [s]						
Water	10	20	30	45	60	75	90
	105	120	150	180	210	360	
Nexbase 3080	120	180	240	300	360	480	600
	720	900	1200	1800			

Table 6: Measuring times

5 Experimental Results

Results of two experimental series are presented in this section, one serie for each of the two liquids. The measured quantities are pressure drop and holdup, both being subject to the large uncertainties discussed in section 4.3, i.e. uncertainties caused by the large error range of the pressure transducers and the uncertainty of the gas flowrates. Flow visualizations taken at the same instants in time as the measurements are included for both experimental series.

5.1 Water

In order to avoid a too large influence of fluctuations in the pressure drop measurements, a 5 second average curve created from four different full dry-up runs are used to extract the pressure drop at the wanted measurements times of Table 6. Figure 18 shows these four runs superimposed, with the 5 second average curve and the measured single phase pressure drop indicated.

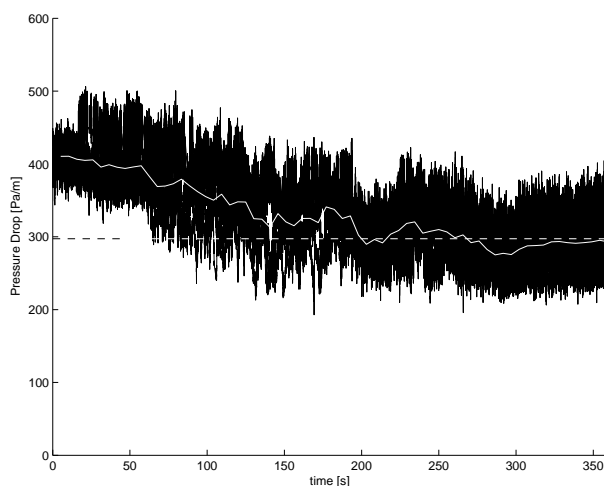


Figure 18: Pressure drop time series of full dry-up runs

The time series of measured pressure drop and holdup are presented in Figure 19 and Figure 20, respectively.

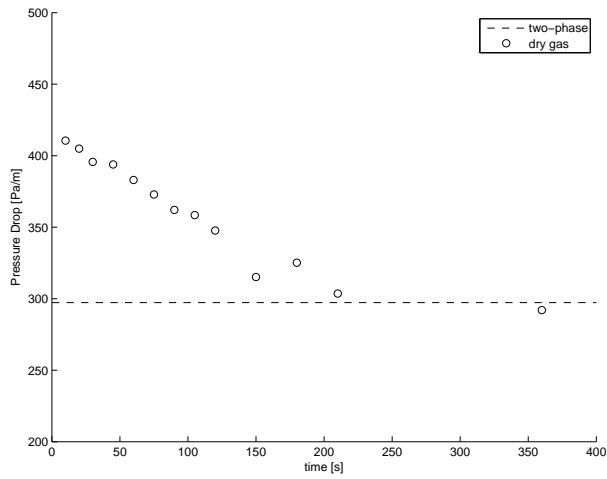


Figure 19: Pressure drop vs. time

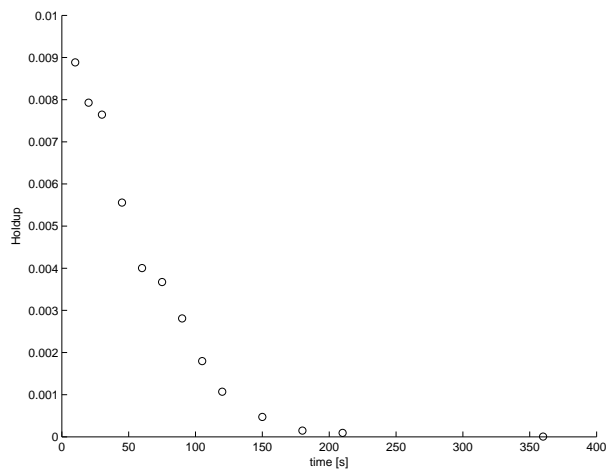


Figure 20: Holdup vs. time

One point in the pressure drop vs. time curve is found to lie below the single phase pressure drop line. However it is likely that this result comes from an uncertainty in the measurements as this is a point corresponding to a completely dry pipe.

A curve showing the measured pressure drop as a function of the measured

holdup is presented in Figure 21. From this figure one can observe a close to linear relation between the measured pressure drop and holdup.

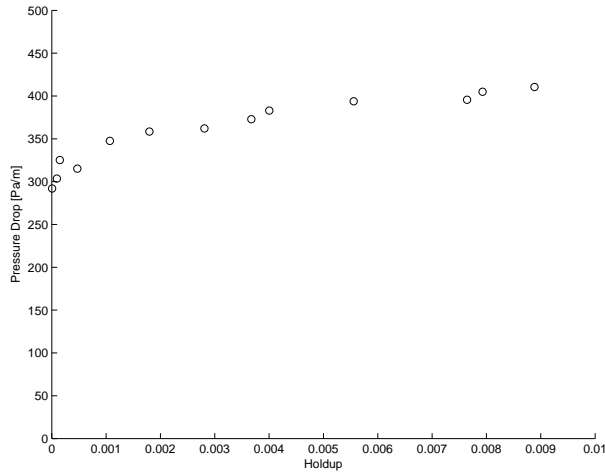


Figure 21: Pressure drop vs. holdup

Flow visualizations of the dry-up process for water as a liquid film are shown in Figures 22 - 34. The visualizations are obtained from the acrylic pipe section, located above the test section, and are taken at the same instants as the pressure drop and holdup measurements. These visualizations show that a liquid film is covering the entire pipe for times up until 75 seconds. Around this time the film breaks down, ripples are observed on the wall. At later times these ripples break down and single droplets are found travelling on the wall. Eventually the pipe is completely dry. A video showing this evolution of the flow is attached electronically in DAIM. The video includes a part of the initial steady flow, while the dry-up process is initiated 2 minutes into the video.



Figure 22: Flow visualization
10 s (air - water)



Figure 23: Flow visualization
20 s (air - water)



Figure 24: Flow visualization
30 s (air - water)



Figure 25: Flow visualization
45 s (air - water)



Figure 26: Flow visualization
60 s (air - water)



Figure 27: Flow visualization
75 s (air - water)



Figure 28: Flow visualization
90 s (air - water)



Figure 29: Flow visualization
105 s (air - water)



Figure 30: Flow visualization
120 s (air - water)



Figure 31: Flow visualization
150 s (air - water)



Figure 32: Flow visualization
180 s (air - water)



Figure 33: Flow visualization
210 s (air - water)



Figure 34: Flow visualization 360 s (air - water)

5.2 Nexbase 3080

In this case, where the high viscosity oil of Nexbase 3080 is used as the liquid film, three different runs of the total dry-up process is used for the extraction of the pressure drop measurements. These runs showed a shape which easily could be represented by an 8^{th} order polynomial, as showed in Figure 35. This 8^{th} order polynomial, white line in Figure 35, gives the pressure drop at the wanted measurement times. In this way fluctuations of the measurements will not produce a too large influence in the measurements.

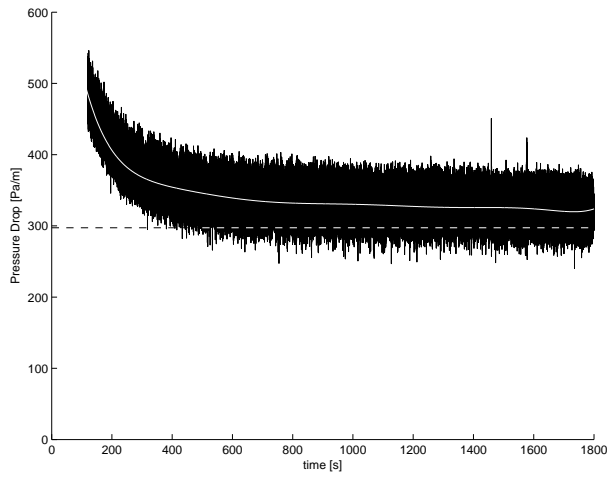


Figure 35: Pressure drop time series of full dry-up runs

Figure 36 and Figure 37 shows the time series of the measured pressure drop and holdup of the Nexbase 3080 experiments.

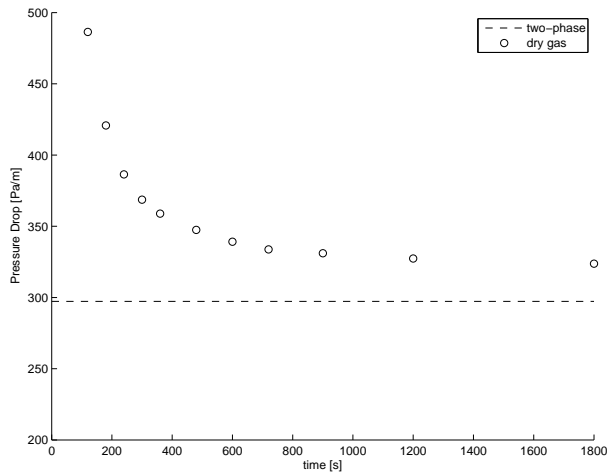


Figure 36: Pressure drop vs. time

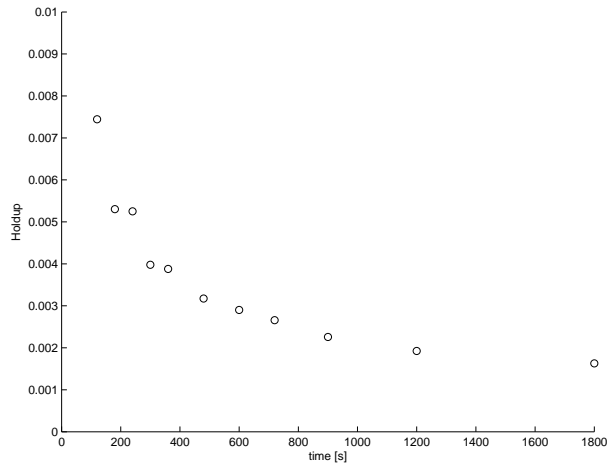


Figure 37: holdup vs. time

The holdup curve and the pressure drop curve show similar shapes, tending towards single phase conditions as time increases. No points in the pressure drop curve is found to lie below the single phase pressure drop.

The pressure drop vs. holdup curve for this case is shown in Figure 38. From this curve the pressure drop looks to have an exponential dependence on the holdup, in the holdup range of these experiments.

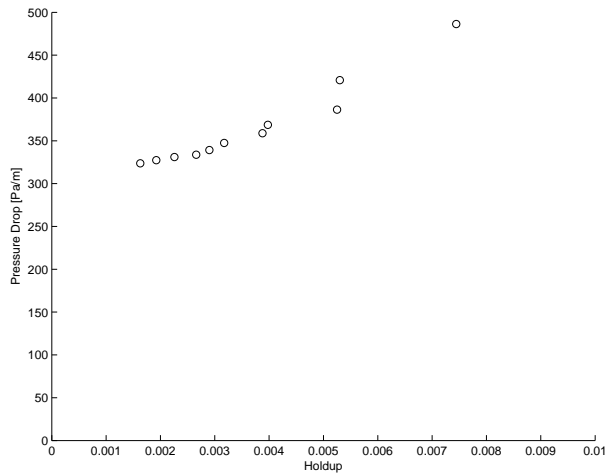


Figure 38: Pressure drop vs. holdup

Figures 39 - 49 shows flow visualizations for all the measurement times. Up until 480 seconds the liquid film was observed to be somewhat equally distributed around the pipe. At later times the film seemed to only cover parts of the pipe. It must be noted that the pipe was never observed to be completely dry, and one part of the pipe wall seemed to keep a thin liquid film even for later times, while the other part seemed dry. This unsymmetrical behaviour are likely a result of the geometry of the setup, but the reason has not been revealed at this point. Videos of the dry-up process is attached electronically in DAIM. One short video is made for each of the experimental points.

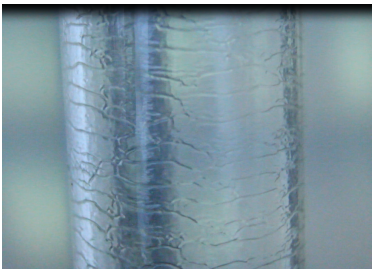


Figure 39: Flow visualization
120 s (air - Nexbase 3080)

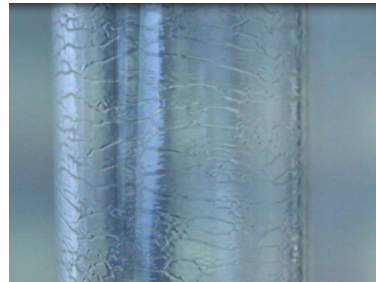


Figure 40: Flow visualization
180 s (air - Nexbase 3080)



Figure 41: Flow visualization
240 s (air - Nexbase 3080)



Figure 42: Flow visualization
300 s (air - Nexbase 3080)



Figure 43: Flow visualization
360 s (air - Nexbase 3080)

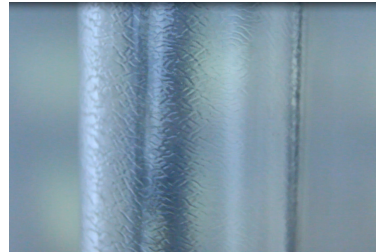


Figure 44: Flow visualization
480 s (air - Nexbase 3080)



Figure 45: Flow visualization
600 s (air - Nexbase 3080)



Figure 46: Flow visualization
720 s (air - Nexbase 3080)



Figure 47: Flow visualization
900 s (air - Nexbase 3080)



Figure 48: Flow visualization
1200 s (air - Nexbase 3080)



Figure 49: Flow visualization 1800 s (air - Nexbase 3080)

5.3 Discussion of experimental results

Due to all the uncertainties related to the experiments performed the values of the pressure drop presented are not of interest. The holdup measurements on the other hand are performed in precise manner, but are extracted from an unknown flow rate of gas. However, as the experiments and measurements have showed good repeatability some conclusions can be drawn about the differences between the two liquids used.

Nexbase 3080 needed much longer time than the water to dry up. In fact the pipes were not observed dry in the oil case, not even in a pre-experimental test run which lasted for 3600 seconds. This difference is not surprising considering the viscosity difference of the two fluids. A comparison of the pressure drop vs. holdup curves, Figure 21 and Figure 38, suggests that a water film produces a lower pressure drop as a function of holdup than for Nexbase 3080, and this difference tends to be larger for increasing values of holdup.

None of the experimental series gave pressure drop measurements below the measured single phase pressure drop. Indicating that the higher viscosity of Nexbase is not sufficient to keep the film stable enough to give the theoretical pressure drop reduction shown in [18]. On the contrary, the pressure drop was observed higher in the oil case than in the water case. It must be noted that only one unknown gas flow rate is used, and that other flow rates might give different results.

6 Simulations

Numerical simulations have been conducted using the two different commercial multiphase simulation softwares OLGA and LedaFlow. The experiments described in [6] are simulated. Because of the earlier described measurement uncertainties of the experiments presented in this thesis, no comparison between the new experiments and simulations are made.

The version of OLGA used in this work is OLGA 7.1. In two-phase cases, as the ones considered here, OLGA uses a two-fluid model where continuity equations are solved for each phase. This model is solved on a fixed grid, using an Eulerian formulation.

LedaFlow Engineering v1.1 is the version used for the LedaFlow simulations. It calculates single, two-phase and three-phase flow using a fully transient 1D model. Mass conservation equations can be solved for continuous and dispersed fields, 9 in total, while equations for enthalpy and energy are solved for continuous phases.

All simulations are performed on a relatively small grid, where every computational cell is of approximately the same size as the pipe diameter. Tests with both smaller and larger grids are performed for all geometries to ensure grid independence.

6.1 Experimental setup

The experiments from [6] were dry-up experiments using air as the gas phase and oil (Exxsol D80) and water as the liquid film. A vertical acrylic pipe with an internal diameter of 0.05 m was used as a test section. Table 7 describes the full geometry of the experimental setup. The horizontal section leading into the vertical parts had in fact an upwards inclination of 2° , which was also included in the simulation geometry.

Description	Length [m]
Horizontal section length	13.46
Total height	6.435
Flow development length	3.740
Test section length	1.69
Pressure measurement distance	1.00
Length of pipe to overflow tank	1.00

Table 7: Geometry of setup

A steady two-phase flow was the initial point of the dry-up process in the experiments, obtained by running gas and liquid for 600 s. At this instant the liquid supply was shut off. Pressure and holdup was measured at different instants until the pipe was dry. In the simulations this procedure was followed, and values for holdup and pressure drop was extracted at approximately the same times as in the experiments. Conditions in the experimental series are listed in Table 8.

Liquid film	Gas phase	U_{SG} [m/s]	U_{SL} [m/s]
Water	Air	30	0.02
Exxsol D80	Air	30	0.02

Table 8: Experimental conditions

6.2 OLGA simulations

Figure 50, Figure 51 and Figure 52 shows a comparison between OLGA simulations and experimental results for the case with water as the liquid film. It must be mentioned that the dry-up processes was initiated faster in the simulations than in the experiments. To ease comparison of the shape of the process the simulation time series have been shifted so that the initial points occur at the same instants of time. This has also been done for the oil case. Also included in the pressure drop - time plots are the dry pipe pressure drop calculated from the pressure drop equation, (15), using the the modified Blasius friction factor, equation (16), and the single phase pressure drop obtained in OLGA.

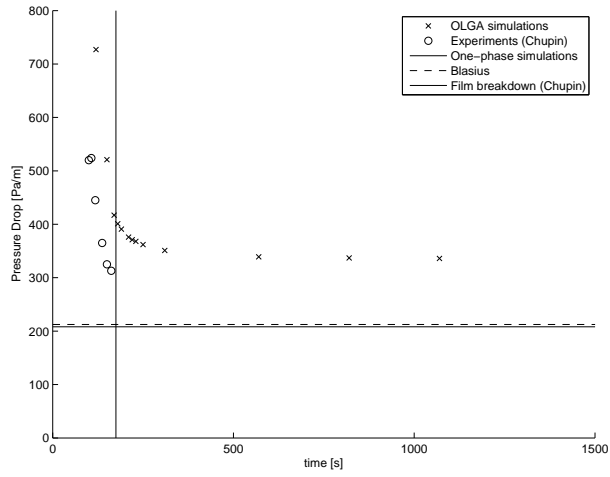


Figure 50: Pressure drop vs. time - Comparison of experiments and OLGA simulation (air - water)

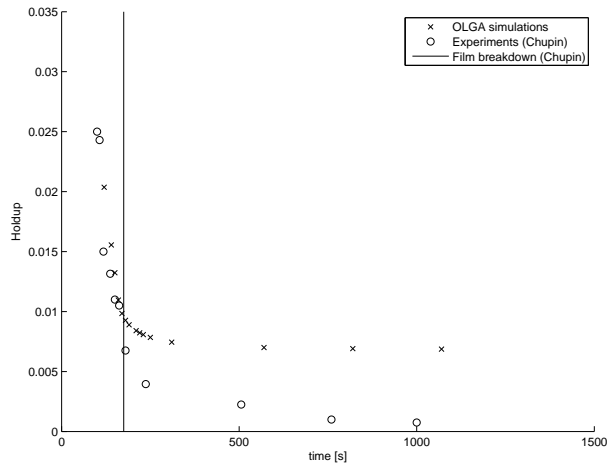


Figure 51: Holdup vs. time - Comparison of experiments and OLGA simulation (air - water)

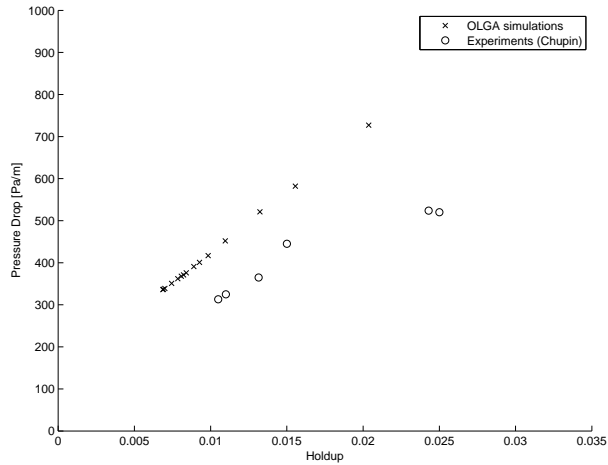


Figure 52: Pressure drop vs. holdup - Comparison of experiments and OLGA simulation (air - water)

The comparisons between simulations and experiments for the Exxsol D80 case is shown in Figure 53, Figure 54 and Figure 55.

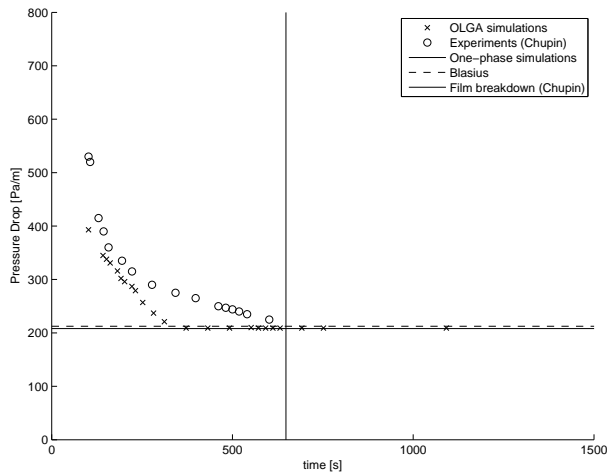


Figure 53: Pressure drop vs. time - Comparison of experiments and OLGA simulation (air - Exxsol D80)

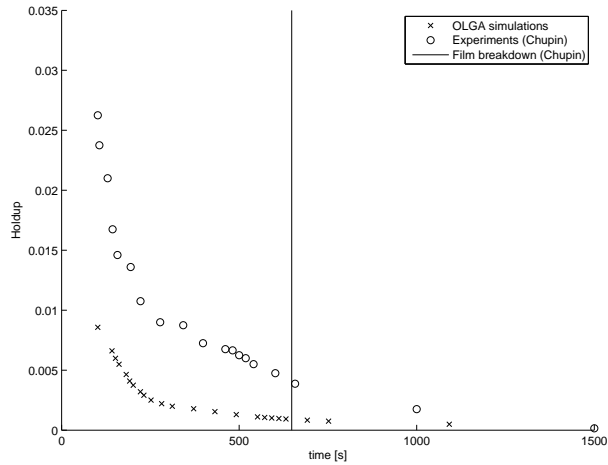


Figure 54: Holdup vs. time - Comparison of experiments and OLGA simulation (air - Exxsol D80)

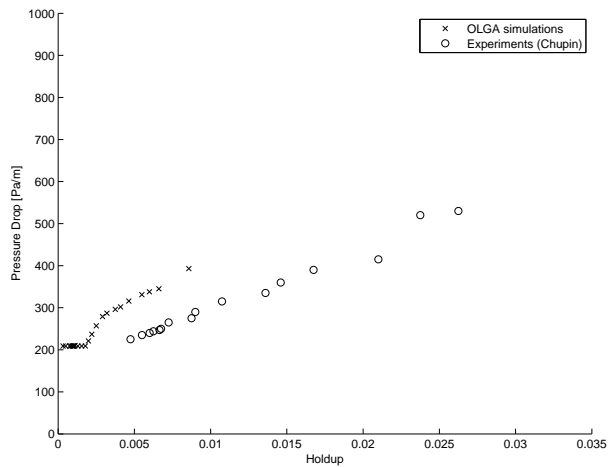


Figure 55: Pressure drop vs. holdup - Comparison of experiments and OLGA simulation (air - Exxsol D80)

From Figure 51 one can observe that the dry-up process, for a liquid film of water, initially behaves similar as in the experiments. However the holdup stabilizes at a non-zero value. In the Exxsol case the holdup is initially much lower

than in the experiments, but approaches zero relatively fast, as can be seen from Figure 54. The pressure drop plots has the same behaviour as their associated holdup plots. For water the simulated pressure drops follows a curve similar as in the experiments for small values of time, but stabilizes at a relatively high value compared to the calculated single phase pressure drop. Simulated pressure drop in the Exxsol case are at first very small, compared to the experiments, but shows a quicker approach to the single phase pressure drop value. OLGA produced quite different results for the two cases, when it comes to the transient dry-up process. In order to check if the pipe becomes dry in the simulated water case, the simulation was runned for a longer time (20000s). This holdup curve is shown in Figure 56. For the ease of comparison, the holdup curve for the Exxsol case is also included in the figure. One can observe that the flow eventually becomes dry also in the case of a liquid film of water. After some time at a non-zero value, the holdup again starts to approach zero. This might indicate a switch of closure models in OLGA, but without further knowledge about OLGA no conclusion about this can be drawn in this thesis.

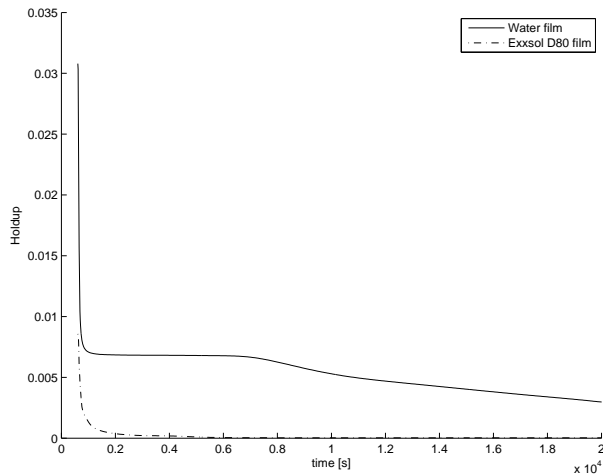


Figure 56: Holdup vs. time - Comparison of dry-up processes in OLGA simulations

If a pressure drop reduction was obtained by the introduction of a liquid film, steady state conditions at where it occurred would be the most valuable results. Therefore the most important curves to investigate is the pressure drop versus holdup curves, Figure 52 and Figure 55. For both liquids used, OLGA overpredicted the pressure drop for a given value of holdup. In the case of a water liquid film the size of errors in the simulations was found to lie between 31% and

43%, while for the case of an Exxsol liquid film these errors were between 34% and 41%. It must be noted that only few points existed at which the holdup values were close enough in the experiments and in the simulations for calculation of errors in the simulation. However by looking at the mentioned plots, the size of the errors intuitively seems to be in the same same range as the ones calculated.

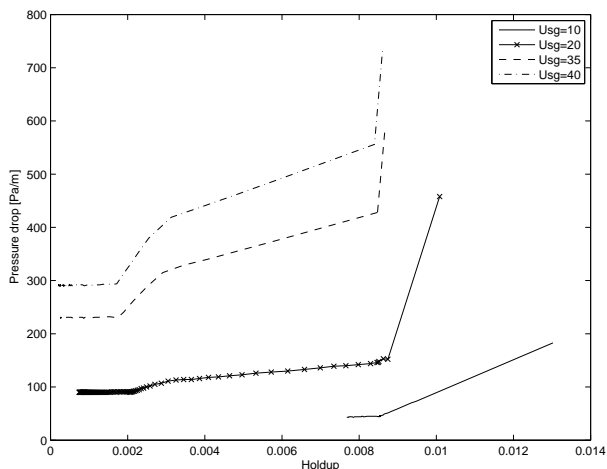
6.3 OLGA parametric study

In order to get a better understanding of how the different parameters are affecting the dry-up process a small parametric study in OLGA has been carried out. In this study one parameter has been altered, compared to experimental conditions, for each simulation. The experiments of Chupin with a liquid film of Exxsol D80 has been simulated. Superficial gas velocity, superficial liquid velocity and viscosity are the parameters investigated. When investigating viscosity, Nexbase 3080 are used to compare with the Exxsol simulation. Table 9 shows which values that are used for the different parameters.

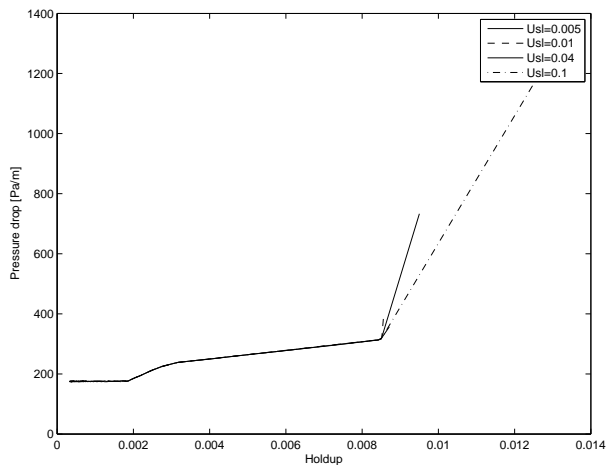
U_{SG} [m/s]	U_{SL} [m/s]	Liquid	ρ_L [kg/m ³]	μ_L [kg/ms]
10	0.005	Exxsol D80	800	$1.79 \cdot 10^{-3}$
20	0.01	Nexbase 3080	833	0.1033
35	0.04			
40	0.1			

Table 9: Parameter values in parameteric study

Figure 57 suggests that the pressure drop increases close to linearly with superficial gas velocity, for a given holdup value, not considering the smallest gas velocity tested. As the gas velocity enters the pressure drop equation in quadratic manner, this would the suggest that OLGA is using an inverse proportional friction factor for annular flows, at least above a certain velocity threshold.

Figure 57: Pressure drop vs. holdup - different U_{SG}

In Figure 58 one can see that the pressure drop is equal for all runs until a certain holdup value. This suggests that the initial liquid amount in dry-up experiments are of little importance, as long as the wanted holdup region is covered. The points causing the sudden changes are corresponding to the instant of time where the liquid supply is shut off, and can therefore probably be neglected in the evaluation the effect of initial superficial liquid velocity.

Figure 58: Pressure drop vs. holdup - different U_{SL}

Viscosity was found to have fairly large impact on the dry-up time. For the end time of the simulations the holdup in the Nexbase 3080 case was far from zero, while in the Exxsol D80 case it approached zero relatively quick. As a consequence of this behaviour, illustrated in Figure 59, equal holdup values for the two cases was not present. However the holdup dependence of the pressure drop seems to be equal for the two cases. Figure 60 shows that the curve for Nexbase 3080 is almost a continuation of the Exxsol D80 curve, indicating that the OLGA friction factor for annular flow is independent of liquid viscosity.

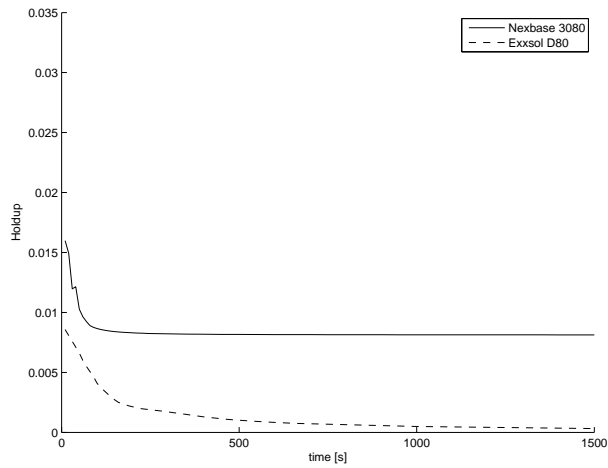


Figure 59: Holdup vs.time - different viscosities

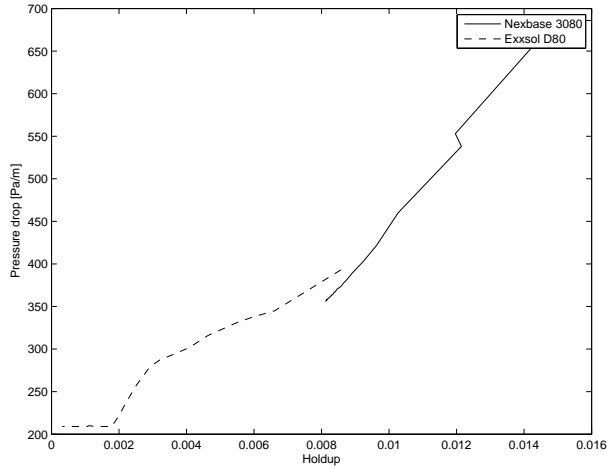


Figure 60: Pressure drop vs. holdup - different viscosities

6.4 LedaFlow simulations

Comparisons between the experiments and the LedaFlow simulations for the water case are shown in Figure 61, Figure 62 and Figure 63. In these simulations the dry-up of liquid was initiated immediately after closing the liquid inlet. The time dependent simulation plots has therefore been shifted in order to compare the transient processes more easily. This is also done in the case of Exxsol D80 as the liquid film, where the comparisons between experiments and simulations are presented in Figure 64, Figure 65 and Figure 66.

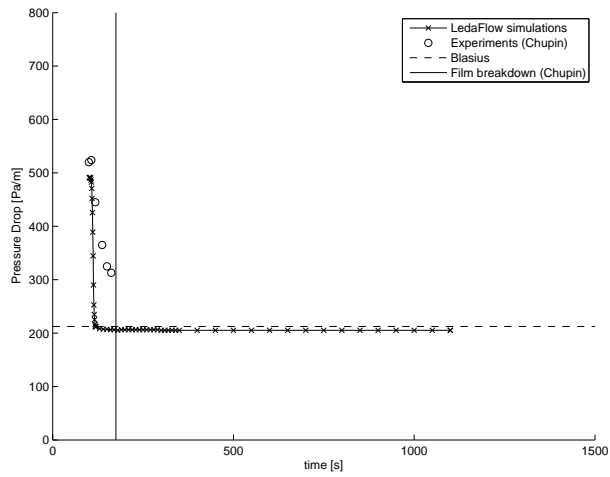


Figure 61: Pressure drop vs. time - Comparison of experiments and LedaFlow simulation (air - water)

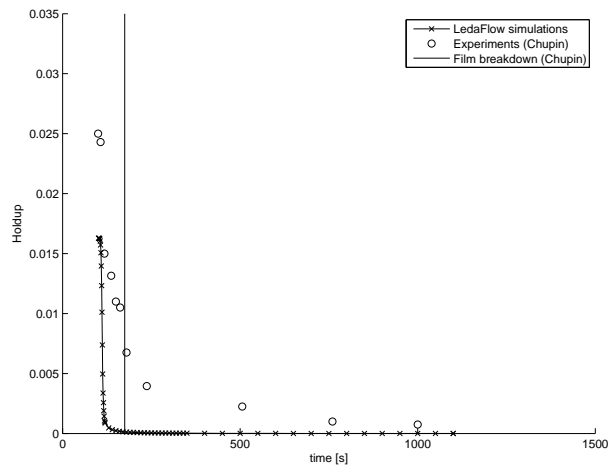


Figure 62: Holdup vs. time - Comparison of experiments and LedaFlow simulation (air - water)

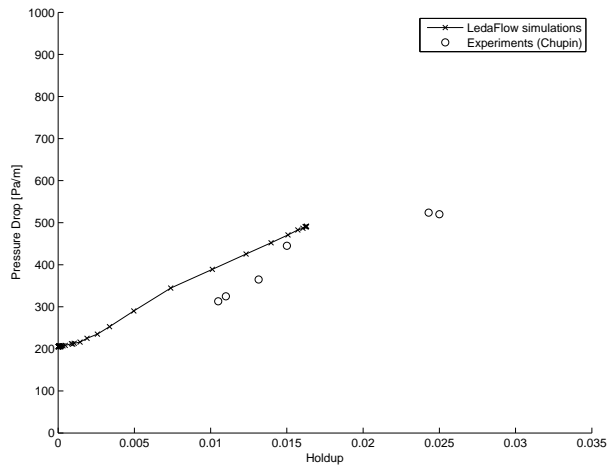


Figure 63: Pressure drop vs. holdup - Comparison of experiments and LedaFlow simulation (air - water)

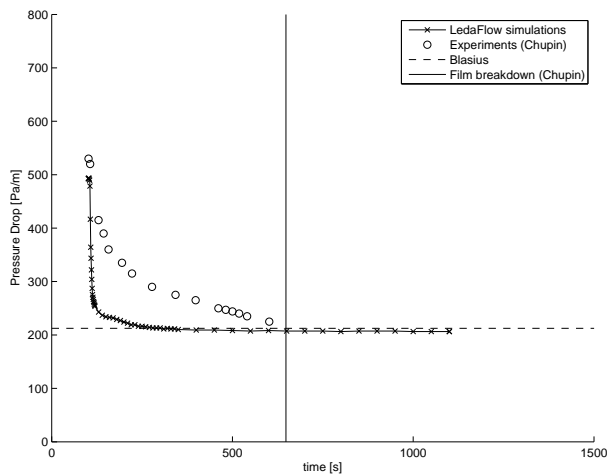


Figure 64: Pressure drop vs. time - Comparison of experiments and LedaFlow simulation (air - Exxsol D80)

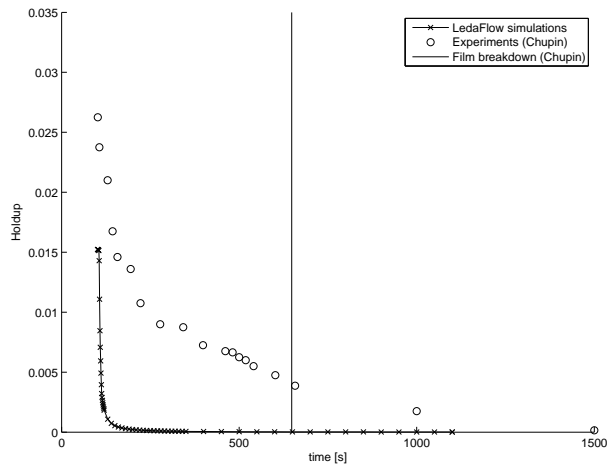


Figure 65: Holdup vs. time - Comparison of experiments and LedaFlow simulation (air - Exxsol D80)

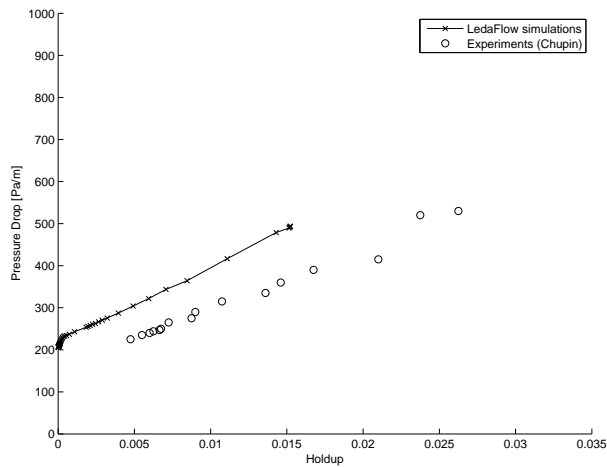


Figure 66: Pressure drop vs. holdup - Comparison of experiments and LedaFlow simulation (air - Exxsol D80)

In the LedaFlow simulations the dry-up of liquid was extremely fast compared to the real dry-up time of the experiments. The holdup goes to zero after only a few seconds, as a result the pressure drop also reaches the dry-gas pressure

drop value, being slightly below the value calculated using the Blasius friction factor, at the same time. Both liquid cases shows similar results in this transient process. At the initial point of the dry up process both simulations produced holdup values below the values observed in the experiments, suggesting that the holdup in LedaFlow are underestimated in the initial steady state flows. However, Figure 61 and Figure 64 shows that the simulated pressure drop is initially close to the experimentally measured pressure drop, for both cases. These observations becomes more evident in the pressure drop - holdup plots, Figure 63 and Figure Figure 66, which shows that LedaFlow overpredicts the pressure drop for given holdup values in these vertical upward flowing annular flow cases. In the case of water as the liquid film this error is in the range of 6% to 24%, while in the Exxsol case the error is found to be in the range of 30% to 35%. It must be noted that also in these LedaFlow simulations only a few points existed, where the holdup was close enough to the experimentally measured holdup values, in order to calculate the error range. However the pressure drop vs. holdup curves suggests that these error ranges are quite reasonable for the whole experimental range.

6.5 Discussion of simulation results

Two series of dry-up experiments of have been simulated with both OLGA and LedaFlow in this section. All of the simulations predicted lower holdup values at the initial point of the process than observed in the experiments. Also the transient dry-up process was predicted to happen much faster in both simulators than reported from experiments. The results of the time dependent processes was quite similar for all of the simulations, with the dry-up process finishing a little quicker in LedaFlow than in OLGA. The one case that showed the most difference in this area was the water case in OLGA, where the holdup stabilized at a non-zero value, before going to zero again at a later point in time.

When it comes to the pressure drop prediction as function of holdup, both simulators was found to overpredict pressure drop. Simulation errors with respect to the experimental points, have been calculated by equation (20), and the error range of each case is listed in table 10. LedaFlow showed throughout to produce a smaller pressure drop error, with respect to holdup, than OLGA. A difference between the errors in the two cases was observed in LedaFlow, which had quite small errors in the water case. The error ranges in OLGA was almost equal for the two liquids used for the film at the wall.

$$E = \left| \frac{x_{measured} - x_{calculated}}{x_{measured}} \right| \quad (20)$$

Simulator	E_{water} [%]	$E_{ExxsolD80}$ [%]
OLGA	31-43	34-41
LedaFlow	6-24	30-35

Table 10: Error ranges in simulations

7 Models for interfacial friction factor

In this chapter, models for interfacial friction factor, presented in Section 3, are compared to experimental data. Table 11 shows the models tested. The interfacial friction factor is included as a closure model in the pressure drop equation, (23). Some of the models include the single phase friction factor on a smooth surface, f_s . Again the friction factor of Blasius, equation (16), for turbulent flows is used for this friction factor. All friction factors tested in this chapter are in the form of the Fanning friction factor, which relates to the shear stress through equation (21). A conversion of the smooth friction factor of equation (16), from Darcy to Fanning representation, has therefore been made by the relation in (22).

$$\tau = \frac{f \rho u^2}{2} \quad (21)$$

$$f_s = \frac{\lambda_s}{4} \quad (22)$$

Name	Model
Wallis (1969)	$f_i = 0.005 \left(1 + 300 \frac{h}{D}\right)$
Hanratty (1991)	$\frac{f_i}{f_s} - 1 = 0.045 \left(\frac{h \rho_G v_G}{\mu_G} - 4\right)$
Fore (2000)	$f_i = 0.005 \left\{1 + 300 \left[\left(1 + \frac{17500}{Re_G}\right) \frac{h}{D} - 0.0015\right]\right\}$
Wallis/Fore (2000)	$f_i = 0.005 \left[1 + 300 \left(\frac{h}{D} - 0.0015\right)\right]$
Henstock (1976)	$f_i = f_s \left(1 + 212 \sqrt{\frac{f_i}{f_s} \frac{h}{D}}\right)$
Asali (1985)	$f_i = f_s \left(1 + 0.45 Re_G^{-0.2} \left(Re_G \sqrt{\frac{f_i}{2} \frac{h}{D}} - 4\right)\right)$

Table 11: Models for f_i found in the literature

As presented in [19], the pressure drop in the gas core of two-phase vertical annular flow can be calculated from equation (23).

$$\frac{dP}{dx} = -\frac{4\tau_i}{D\sqrt{1-H}} - \rho_G g \quad (23)$$

where

$$\tau_i = \frac{1}{2} f_i \rho_G u_G^2 \quad (24)$$

These two relations, together with the models in Table 11 are used to predict the pressure drop as a function of holdup. Fixed point iterations are used when

the models are iterative. In Figure 67, Figure 68, Figure 69 and Figure 70 comparisons between the models and the experiments presented in [6] are shown. Because of the explained measurement uncertainties, models have not been tested against the new experiments presented in this thesis. The performance of the models is summarized in Table 12, showing the range of error of the models in each of the cases. Errors are calculated using equation (20).

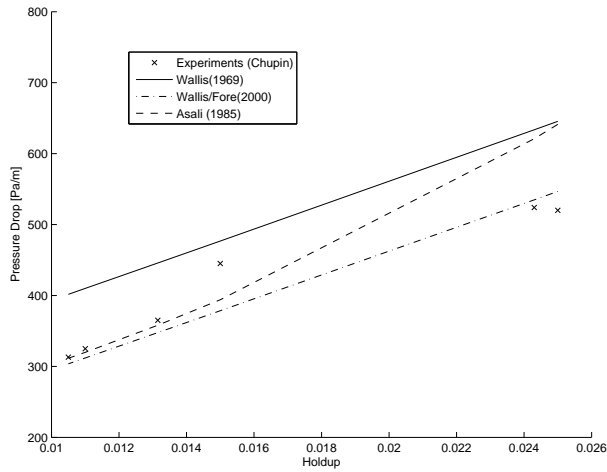


Figure 67: Pressure drop vs. holdup - Comparison of experiments (Chupin) and interfacial friction factor models (air - water)

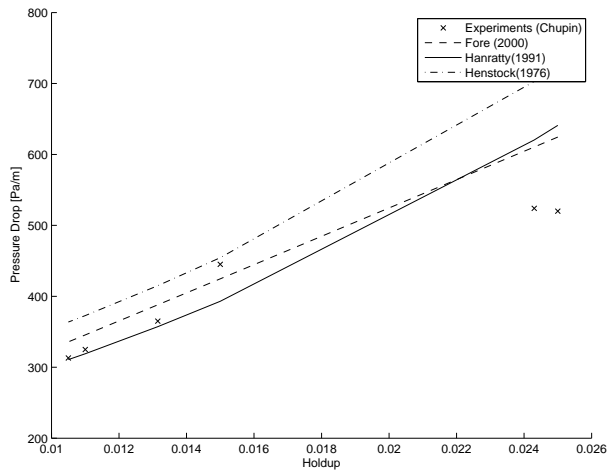


Figure 68: Pressure drop vs. holdup - Comparison of experiments (Chupin) and interfacial friction factor models (air - water)

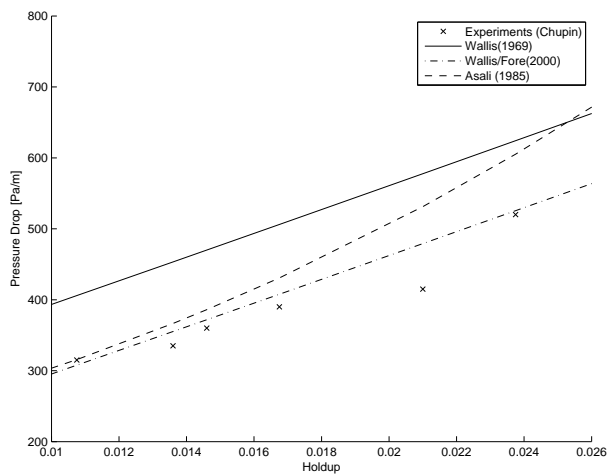


Figure 69: Pressure drop vs. holdup - Comparison of experiments (Chupin) and interfacial friction factor models (air - Exxsol D80)

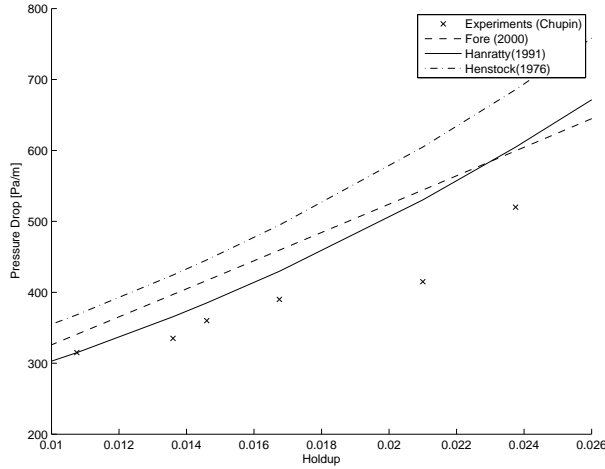


Figure 70: Pressure drop vs. holdup - Comparison of experiments (Chupin) and interfacial friction factor models (air - Exxsol D80)

Model	$E_{water}[\%]$	$E_{ExxsolD80}[\%]$
Wallis (1969)	7-28	20-39
Hanratty (1991)	0.7-23	0-28
Fore (2000)	5-20	1-31
Wallis/Fore (2000)	3-15	0.1-15
Henstock (1976)	2-39	16-46
Asali (1985)	0.5-23	0.2-28

Table 12: Error ranges for friction factor correlations

Most of the models are showing the best results at the smallest holdup values in both cases. The one exception of this trend is the Wallis factor which shows a consistent overprediction of the pressure drop for all the holdup values in the experiments. The pressure drop - holdup curve flattens out in the water experiments, a behaviour not reproduced in any of the models. Some of the models are linear with respect to holdup, and are therefore following the linear shape of observed in the Exxsol D80 experiments. However, almost all of them are overpredicting the pressure drop. The models of Asali(1985), Hanratty(1991) and Henstock(1976) all shows a greater slope at larger holdups. This trend is wrong compared to the experimental data, especially in the case of a water liquid film. When it comes to the best fit considering all of the experimental points, the

model of Wallis/Fore(2000) stands out as the best for both cases. Not suprisingly considering the quite small holdup values in these experiments, and this model only being a shift in the friction factor of Wallis(1969), made to tune it better for small values of holdup.

8 Conclusion

The work presented in this thesis is a continuation of the experimental investigations in [6], on the theoretical possibility of pressure drop reductions in gas transport pipelines presented in [18].

In order to investigate this possible pressure drop reduction, an experimental setup was built in the multiphase laboratory. Two different fluids were used as liquid film, water and the high viscosity oil Nexbase 3080. Holdup and pressure drop measurements were made at different instants in time during a dry-up process, where air was blown, with a close to constant rate, over an initial liquid film, which became thinner with increasing time, before breaking down. One experimental serie was made for each of the liquids. Due to large uncertainties in both the value of the gas flow rate and in the pressure drop measurements, the experimental results can only serve as indications on how the pressure drop depends on the liquid holdup compared to measured single phase conditions. Simulations of the similar experiments, performed earlier at NTNU and presented in [6], were performed in both OLGA and LedaFlow. These experimental results, obtained using water and Exxsol D80 as liquid films, were also compared with pressure drop calculations using different models for the interfacial friction factor, found in the literature.

No indications of a pressure drop reduction, by introduction a liquid film on the wall, was observed in the experiments. On the contrary the pressure drop was observed to rise with increasing holdup values. Many researches in the field of turbulent gas flow over a liquid film, adresses this extra pressure drop to waves on the gas-liquid interface. Flow visualizations shows that waves were present on the interface for both liquids used, and the introduction of a liquid film of high viscosity did not result in a smooth gas-liquid interface in the experiments performed. When comparing water and Nexbase 3080 as liquid films, water was found to give a smaller pressure drop than Nexbase 3080, at given holdup values.

All simulations performed overpredicted the pressure drop for given holdups. However, both simulation softwares were able to follow the shape of these curves in a somewhat reasonable matter. Most of the interfacial friction factor models were also found to overpredict the pressure drop, especially for the larger part of the holdup range of the experiments. The model of Wallis/Fore (2000) distinguished itself from the rest by clearly providing the best fit of all the experimental points, for both cases.

Due to the large uncertainties in the experimental results, it is not found relevant to present this work through a publication.

Some recommendations for further work are listed below:

- Repetition of the experiments presented in this thesis using a differential

pressure transducer with an appropriate range, in order to present accurate data on the phenomena. For this the problem associated with the flow rate of air must be solved in advance.

- Address the cause of the unsymmetrical behaviour of the Nexbase 3080 film in the experiments.
- Investigate experimentally if the gas-liquid interface could be kept smooth using different air flowrates and liquid amounts, using the high viscosity oil Nexbase 3080.
- Due to the large scale of the possible energy savings caused by reducing the pressure drop in gas transport pipelines, new experimental efforts to obtain smooth gas-liquid interfaces could be made, using different fluids.

References

- [1] Engineering toolbox. <http://www.engineeringtoolbox.com>.
- [2] J. C. Asali and T. J. Hanratty. Ripples generated on a liquid film at high gas velocities. *Int. J. Multiphase Flow*, 19:229–243, 1993.
- [3] J. C. Asali, T. J. Hanratty, and P. Andreussi. Interfacial drag and film height for vertical annular flow. *AIChE Journal*, 31:895–902, 1985.
- [4] B. Asante. Two phase flow: Accounting for the presence of liquids in gas pipeline simulation. In *International Pipeline Conference*, 2004.
- [5] R. J. Belt. *On the liquid film in inclined annular flow*. PhD thesis, Delft University of Technology, 2007.
- [6] G. Chupin. *An experimental investigation of multiphase gas-liquid pipe flow at low liquid loading*. PhD thesis, NTNU, 2003.
- [7] G. Chupin and O. J. Nydal. Drag reduction in gas transport pipelines. Technical report, NTNU, 2002.
- [8] G. Chupin and O. J. Nydal. Terms of the pressure drop equation in gas/condensate pipe flow. Technical report, NTNU, 2002.
- [9] G. Chupin and O. J. Nydal. Three-phase pipe flow experiments at low liquid loading. Technical report, NTNU, 2002.
- [10] L. S. Cohen and T. J. Hanratty. Effect of waves at a gas-liquid interface on a turbulent air flow. *J. Fluid Mech.*, 31:467–479, 1968.
- [11] A. D. D. Craik. Wind-generated waves in thin liquid films. *J. Fluid Mech.*, 26:369–392, 1966.
- [12] L. B. Fore, S. G. Beus, and R. C. Bauer. Interfacial friction in gas-liquid annular flow: analogies to full and transition roughness. *Int. J. Multiphase Flow*, 26:1755–1769, 2000.
- [13] T. J. Hanratty. Separated flow modelling and interfacial transport phenomena. *Applied Scientific Research*, 48:353–390, 1991.
- [14] T. J. Hanratty and J. M. Engen. Interaction between a turbulent air stream and a moving water surface. *A.I.Ch.E. Journal*, 3:299–304, 1957.
- [15] W. H. Henstock and T. J. Hanratty. The interfacial drag and the height of the wall layer in annular flows. *AIChE Journal*, 22:990–1000, 1976.

- [16] G. F. Hewitt and P.M. Lacey. The breakdown of the liquid film in annular two-phase flow. *Int. J. Heat Mass Transfer*, 8:781–791, 1965.
- [17] I. Eskerud Smith, F. N. Krampa, M. Fossen, C. Brekken, and T. E. Unander. Investigation of horizontal two-phase gas-liquid pipe flow using high viscosity oil: Comparison with experiments using low viscosity oil and simulations. *15th International Conference on Multiphase production Technology, Cannes, France*, pages 293–307, 2011.
- [18] S. Solbakken and H. I. Andersson. Turbulent pipe flow with a laminar liquid film at the wall. Technical report, NTNU, 2000.
- [19] G.B. Wallis. *One-dimensional two-phase flow*. McGraw-Hill, 1969.
- [20] F. M. White. *Fluid Mechanics*. McGraw-Hill Higher Education, 1979.

Nomenclature

A	cross sectional area
A_C	cross sectional area of gas core
D	internal pipe diameter
H	liquid holdup
P_C	perimeter of the gas core
Re	Reynolds number
Re_G	gas Reynolds number
Re_L	liquid Reynolds number
S	pipe perimeter
U_B	bulk velocity
U_{SG}	superficial velocity of gas
U_{SL}	superficial velocity of liquid
\dot{V}	volume flow rate
λ_s	single phase friction factor (Darcy)
μ_{Cw}	velocity of roll waves
μ_G	dynamic viscosity of gas
ρ	density
ρ_m	mixture density
ρ_G	gas density
$\sigma_{g/l}$	Surface tension between air and liquid
σ_x	standard deviation of x
\sim	scaling with
θ	Pipe inclination
f_i	interfacial friction factor

f_s	smooth wall friction
g	gravitational constant
h	mean film thickness
p	pressure
v_G	friction velocity of gas
\bar{x}	mean value of x
E	Error
L	Length
Le	Development length
m	mass
Re	Reynolds number
V	volume

Appendices

A PVT file - water

```
'ENTROPY 'air_water EOS= SRK
2 2
4.99990E+06 .400000E+01
.100000E+03 .180000E+02
.100000E+10 .100000E+10
.000000E+00 .000000E+00
GAS DENSITY (KG/M3)
1.1968E-03 1.1806E-03
5.984E+01 5.9029E+01
LIQUID DENSITY (KG/M3)
9.98E+02 9.98E+02
9.98E+02 9.98E+02
DRHOG/DP (S2/M2)
1.1968E-05 1.1806E-05
1.1968E-05 1.1806E-05
DRHOL/DP (S2/M2)
0.0 0.0
0.0 0.0
DRHOG/DT (KG/M3/K)
-4.111E-06 -3.9999E-06
-2.0553E-01 -1.99998E-01
DRHOL/DT (KG/M3/K)
0.0 0.0
0.0 0.0
GAS MASS FRACTION (-)
.100000E+01 .100000E+01
.100000E+01 .100000E+01
GAS VISCOSITY (NS/M2)
1.82500E-05 1.82500E-05
1.82500E-05 1.82500E-05
LIQUID VISCOSITY (NS/M2)
1.00200E-03 1.00200E-03
1.00200E-03 1.00200E-03
GAS HEAT CAPACITY (J/KG/K)
.100700E+04 .100700E+04
.100700E+04 .100700E+04
LIQUID HEAT CAPACITY (J/KG/K)
.418200E+04 .418200E+04
.418200E+04 .418200E+04
GAS ENTHALPY (J/KG)
1.0 1.0
```


1.0	1.0
LIQUID ENTHALPY (J/KG)	
1.0	1.0
1.0	1.0
GAS THERMAL CONDUCTIVITY (W/M/K)	
2.514000E-02	2.514000E-02
2.514000E-02	2.514000E-02
LIQUID THERMAL CONDUCTIVITY (W/M/K)	
5.980000E-01	5.980000E-01
5.980000E-01	5.980000E-01
SURFACE TENSION (N/M)	
7.290000E-02	7.290000E-02
7.290000E-02	7.290000E-02
GAS ENTROPY (J/KG/C)	
0.0	0.0
0.0	0.0
LIQUID ENTROPY (J/KG/C)	
0.0	0.0
0.0	0.0

B PVT file - Exxsol D80

'fdffd'

2 2

4.999900e+006 0.100000e+002

1.000000e+002 0.150000e+002

.100000E+10 .100000E+10

.000000E+00 .000000E+00

GAS DENSITY (KG/M3)

0.001209260e+000 0.001168700e+000

6.046302000e+001 5.843508300e+001

LIQUID DENSITY (KG/M3)

8.000000e+002 8.000000e+002

8.000000e+002 8.000000e+002

PRES. DERIV. OF GAS DENS.

1.209260e-005 1.168700e-005

1.209260e-005 1.168700e-005

PRES. DERIV. OF LIQUID DENS.

0.000000e+000 0.000000e+000

0.000000e+000 0.000000e+000

TEMP. DERIV. OF GAS DENS.

-4.19660e-006 -3.91980e-006

-0.20980e+000 -0.19600e+000

TEMP. DERIV. OF LIQUID DENS.

0.000000e+000 0.000000e+000

0.000000e+000 0.000000e+000

GAS MASS FRACTION OF GAS + OIL

1.000000e+000 1.000000e+000

1.000000e+000 1.000000e+000

GAS VISCOSITY (N S/M2)

1.820000e-005 1.820000e-005

1.820000e-005 1.820000e-005

LIQ. VISCOSITY (N S/M2)

1.790000e-003 1.790000e-003

1.790000e-003 1.790000e-003

GAS SPECIFIC HEAT (J/KG K)

1.000000e+000 1.000000e+000

1.000000e+000 1.000000e+000

LIQ. SPECIFIC HEAT (J/KG K)

1.000000e+000 1.000000e+000

1.000000e+000 1.000000e+000

GAS ENTHALPY (J/KG)

1.000000e+000 1.000000e+000

1.000000e+000 1.000000e+000
LIQ. ENTHALPY (J/KG)
1.000000e+000 1.000000e+000
1.000000e+000 1.000000e+000
GAS THERMAL COND. (W/M K)
1.000000e+000 1.000000e+000
1.000000e+000 1.000000e+000
LIQ. THERMAL COND. (W/M K)
1.000000e+000 1.000000e+000
1.000000e+000 1.000000e+000
SURFACE TENSION GAS/OIL (N/M)
0.024600e-002 0.024600e-002
0.024600e-002 0.024600e-002
GAS ENTROPY (J/KG/C)
0.000000e+000 0.000000e+000
0.000000e+000 0.000000e+000
LIQUID ENTROPY (J/KG/C)
0.000000e+000 0.000000e+000
0.000000e+000 0.000000e+000

C PVT file - Nexbase 3080

'fdffd'

2 2 .609056E+00
4.999900e+006 0.1000000e+002
1.000000e+002 0.1500000e+002
.100000E+10 .100000E+10
.000000E+00 .000000E+00
GAS DENSITY (KG/M3)
0.001209260e+000 0.001168700e+000
6.046302000e+001 5.843508300e+001
LIQUID DENSITY (KG/M3)
8.330000e+002 8.330000e+002
8.330000e+002 8.330000e+002
PRES. DERIV. OF GAS DENS.
1.209260e-005 1.168700e-005
1.209260e-005 1.168700e-005
PRES. DERIV. OF LIQUID DENS.
0.000000e+000 0.000000e+000
0.000000e+000 0.000000e+000
TEMP. DERIV. OF GAS DENS.
-4.196600e-006 -3.919800e-006
-0.209800e+000 -0.196000e+000
TEMP. DERIV. OF LIQUID DENS.
0.000000e+000 0.000000e+000
0.000000e+000 0.000000e+000
GAS MASS FRACTION OF GAS + OIL
1.000000e+000 1.000000e+000
1.000000e+000 1.000000e+000
GAS VISCOSITY (N S/M2)
1.825000e-005 1.825000e-005
1.825000e-005 1.825000e-005
LIQ. VISCOSITY (N S/M2)
0.103300e+000 0.103300e+000
0.103300e+000 0.103300e+000
GAS SPECIFIC HEAT (J/KG K)
0.000000e+000 0.000000e+000
0.000000e+000 0.000000e+000
LIQ. SPECIFIC HEAT (J/KG K)
0.000000e+000 0.000000e+000
0.000000e+000 0.000000e+000
GAS ENTHALPY (J/KG)
0.000000e+000 0.000000e+000

0.000000e+000 0.000000e+000
LIQ. ENTHALPY (J/KG)
0.000000e+000 0.000000e+000
0.000000e+000 0.000000e+000
GAS THERMAL COND. (W/M K)
0.000000e+000 0.000000e+000
0.000000e+000 0.000000e+000
LIQ. THERMAL COND. (W/M K)
0.000000e+000 0.000000e+000
0.000000e+000 0.000000e+000
SURFACE TENSION GAS/OIL (N/M)
2.070000e-002 2.070000e-002
2.070000e-002 2.070000e-002
GAS ENTROPY (J/KG/C)
0.000000e+000 0.000000e+000
0.000000e+000 0.000000e+000
LIQUID ENTROPY (J/KG/C)
0.000000e+000 0.000000e+000
0.000000e+000 0.000000e+000

D Risikovurderingsrapport

Risikovurderingsrapport

Gas Flow in Vertical Pipe with Wet Walls

Prosjekttittel	Experiments on Gas Flow With Wet Pipe Walls
Prosjektleder	Ole Jørgen Nydal
Enhet	NTNU
HMS-koordinator	Erik Langørgen
Linjeleder	Olav Bolland
Plassering	VATL- Flerfaselab
Romnummer	C164
Riggansvarlig	Andrea shmueli, Thomas Arnulf
Risikovurdering utført av	Thomas Arnulf

INNHALDSFORTEGNELSE

1	INNLEDNING	1
2	ORGANISERING	1
3	RISIKOSTYRING AV PROSJEKTET	1
4	TEGNINGER, FOTO, BESKRIVELSER AV FORSØKSOPPSETT	1
5	EVAKUERING FRA FORSØKSOPPSETNINGEN.....	2
6	VARSLING	2
6.1	Før forsøkskjøring	2
6.2	Ved uønskede hendelser.....	2
7	VURDERING AV TEKNISK SIKKERHET	3
7.1	Fareidentifikasjon, HAZOP	3
7.2	Brannfarlig, reaksjonsfarlig og trykksatt stoff og gass	3
7.3	Trykkpåkjent utstyr	3
7.4	Påvirkning av ytre miljø (utslipp til luft/vann, støy, temperatur, rystelser, lukt).....	3
7.5	Stråling	4
7.6	Bruk og behandling av kjemikalier	4
7.7	El sikkerhet (behov for å avvike fra gjeldende forskrifter og normer)	4
8	VURDERING AV OPERASJONELL SIKKERHET.....	4
8.1	Prosedyre HAZOP	4
8.2	Drifts og nødstopps prosedyre.....	4
8.3	Opplæring av operatører	4
8.4	Tekniske modifikasjoner	4
8.5	Personlig verneutstyr	5
8.6	Generelt	5
8.7	Sikkerhetsutrustning	5
8.8	Spesielle tiltak	5
9	TALLFESTING AV RESTRISIKO – RISIKOMATRISJE	5
10	KONKLUSJON	5
11	LOVER FORSKRIFTER OG PÅLEGG SOM GJELDER	6
12	DOKUMENTASJON	6
13	VEILEDNING TIL RAPPORTMAL	7

1 INNLEDNING

Beskrivelse av forsøksoppsetningen og formålet med eksperimentene. Hvor er riggen plassert?

2 ORGANISERING

Rolle	NTNU	Sintef
Lab Ansvarlig:	Morten Grønli	Harald Mæhlum
Linjeleder:	Olav Bolland	Lars Sørum
HMS ansvarlig:	Olav Bolland	Lars Sørum
HMS koordinator	Erik Langørgen	Harald Mæhlum
HMS koordinator	Bård Brandåstrø	
Romansvarlig:	Martin Bustadmo	
Prosjektleder:	Ole Jørgen Nydal	
Ansvarlig riggoperatører:	Thomas Arnulf, Andrea Shmueli	

3 RISIKOSTYRING AV PROSJEKTET

Hovedaktiviteter risikostyring	Nødvendige tiltak, dokumentasjon	DTG
Prosjekt initiering	Prosjekt initiering mal	13.05.2013
Veiledningsmøte	Skjema for Veiledningsmøte med pre-risikovurdering	13.05.2013
Innledende risikovurdering	Fareidentifikasjon – HAZID Skjema grovanalyse	13.05.2013
Vurdering av teknisk sikkerhet	Prosess-HAZOP Tekniske dokumentasjoner	13.05.2013
Vurdering av operasjonell sikkerhet	Prosedyre-HAZOP Opplæringsplan for operatører	13.05.2013
Sluttvurdering, kvalitetssikring	Uavhengig kontroll Utstedelse av apparaturkort Utstedelse av forsøk pågår kort	13.05.2013

4 TEGNINGER, FOTO, BESKRIVELSER AV FORSØKSOPPSETT

Vedlegg:

Prosess og Instrumenterings Diagram (PID)

Luft fra det sentrale systemet strømmer igjennom oppsettet og ut i utløpstanken i flerfaselaben. Derfra slippes luften ut til omgivelsene. Vann eller olje vil introduseres i små mengder, slik at det dannes en væskefilm på rørveggen i den vertikale testseksjonen. Ved bestemte tidspunkt vil ventiler på hver side av testseksjonen lukkes. Væskemengden vil på disse tidspunkt måles ved å tømme seksjonen og væsken samles og veies. Lufttilførselen sperres automatisk før ventilen stenges, slik at en trykkoppygning ikke kan finne sted.

5 EVAKUERING FRA FORSØKSOPPSETNINGEN

Evakuering skjer på signal fra alarmklokker eller lokale gassalarmstasjon med egen lokal varsling med lyd og lys utenfor aktuelle rom, se 6.2

Evakuering fra rigg området foregår igjennom merkede nødutganger til møteplass, (hjørnet gamle kjemi/kjelhuset eller parkeringsplass 1a-b.)

Aksjon på rigg ved evakuering: *Pumpen skal slås av ved nødstopknappen. Ventil ?? skal lukkes manuelt.*

6 VARSLING

6.1 Før forsøkskjøring

Varsling per e-post, til iept-experiments@ivt.ntnu.no

I e-posten skal det stå::

- Navn på forsøksleder:
- Navn på forsøksrigg:
- Tid for start: (dato og klokkeslett)
- Tid for stop: (dato og klokkeslett)

All forsøkskjøringen skal planlegges og legges inn i aktivitetskalender for lab. Forsøksleder må få bekreftelse på at forsøkene er klarert med øvrig labdrift før forsøk kan iverksettes.

6.2 Ved uønskede hendelser

BRANN

Ved brann en ikke selv er i stand til å slukke med rimelige lokalt tilgjengelige slukkemidler, skal nærmeste brannalarm utløses og arealet evakueres raskest mulig. En skal så være tilgjengelig for brannvesen/bygningsvaktmester for å påvise brannsted.

Om mulig varsles så:

NTNU	SINTEF
Labsjef Morten Grønli, tlf: 918 97 515	Labsjef Harald Mæhlum tlf 930 14 986
HMS: Erik Langørgen, tlf: 918 97 160	Forskningsjef Lars Sørum tlf: 928 04 925
Instituttleder: Olav Bolland: 918 97 209	
NTNU – Sintef Beredskapstelefon	800 80 388

GASSALARM

Ved gassalarm skal gassflasker stenges umiddelbart og området ventileres. Klarer man ikke innen rimelig tid å få ned nivået på gasskonsentrasjonen så utløses brannalarm og laben evakueres. Dedikert personell og eller brannvesen sjekker så lekkasjested for å fastslå om det er mulig å tette lekkasje og lufte ut området på en forsvarlig måte.

Varslingsrekkefølge som i overstående punkt.

PERSONSKADE

- Førstehjelpsutstyr i Brann/førstehjelpsstasjoner,
- Rop på hjelp,
- Start livreddende førstehjelp
- **Ring 113** hvis det er eller det er tvil om det er alvorlig skade.

ANDRE UØNSKEDE HENDELSER (AVVIK)

NTNU:

Rapportering av uønskede hendelser, Innsida, avviksmeldinger
https://innsida.ntnu.no/lenkesamling_vis.php?katid=1398

SINTEF:

Synergi

7 VURDERING AV TEKNISK SIKKERHET

7.1 Fareidentifikasjon, HAZOP

Se kapittel 13 "Veiledning til rapport mal.

Forsøksoppsetningen deles inn i følgende noder:

Node 1	
Node 2	
Node 3	

Vedlegg, skjema: Hazop_mal

Vurdering: Sikkerheten er ivaretatt. Skadeomfanget av uforutsette hendelser begrenses av nødstopknappen

7.2 Brannfarlig, reaksjonsfarlig og trykksatt stoff og gass

Se kapittel 13 "Veiledning til rapport mal.

Inneholder forsøkene brannfarlig, reaksjonsfarlig og trykksatt stoff

JA	Antennestemperatur er ??C for Nexbase 3080
----	--

Vurdering: *Oljene må håndteres som brennbare stoff, Datablad for oljen finnes ved operatørplass.*

7.3 Trykkpåkjent utstyr

Inneholder forsøksoppsetningen trykkpåkjent utstyr:

NEI	
-----	--

Trykkutsatt utstyr skal trykktestes med driftstrykk gange faktor 1.4, for utstyr som har usertifiserte sveiser er faktoren 1.8. Trykktesten skal dokumenteres skriftlig hvor fremgangsmåte framgår.

Vurdering: Forsøkene utføres rundt atmosfærisk trykk. Trykkoppbygning vil kun kunne forekomme etter lukking av ventilene, oppstrøms for ventilene. Lufttilførsel stenges av automatisk rett før (100ms) ventilene lukker seg, for å forhindre trykkoppbygning.

7.4 Påvirkning av ytre miljø (utslipp til luft/vann, støy, temperatur, rystelser, lukt)

Se kapittel 13 "Veiledning til rapport mal.

JA	Lekkasje fra oppsettet vil medføre glatte gulv
----	--

Vurdering: Oppsettet er sjekket for lekkasjer. Vær nøye med ikke å avhende olje i avløpet, oljen skal oppbevares i passende fat.

7.5 Stråling

Se kapittel 13 "Veiledning til rapport mal.

NEI	
-----	--

7.6 Bruk og behandling av kjemikalier

Se kapittel 13 "Veiledning til rapport mal.

JA	Nexbase 3080
----	--------------

Vurdering: Datablad finnes ved operatørplass

7.7 El sikkerhet (behov for å avvike fra gjeldende forskrifter og normer)

NEI	
-----	--

8 VURDERING AV OPERASJONELL SIKKERHET

Sikrer at etablerte prosedyrer dekker alle identifiserte risikoforhold som må håndteres gjennom operasjonelle barrierer og at operatører og teknisk utførende har tilstrekkelig kompetanse.

8.1 Prosedyre HAZOP

Se kapittel 13 "Veiledning til rapport mal.

Metoden er en undersøkelse av operasjonsprosedyrer, og identifiserer årsaker og farekilder for operasjonelle problemer.

Vedlegg: HAZOP_MAL_Pro prosedyre

Vurdering: Prosedyren er enkel og feil vil ikke skape uakseptable situasjoner.

8.2 Drifts og nødstopps prosedyre

Se kapittel 13 "Veiledning til rapport mal.

Driftsprosedyren er en sjekklister som skal fylles ut for hvert forsøk.

Nødstopps prosedyren skal sette forsøksoppsetningen i en harmløs tilstand ved uforutsette hendelser.

Vedlegg: "Procedure for running experiments"

Nødstopps prosedyre: Pumpen skal skrues av ved nødknapp. Ventil ?? skal lukkes manuelt.

8.3 Opplæring av operatører

Dokument som viser Opplæringsplan for operatører utarbeides for alle forsøksoppsetninger.

- *Hvilke krav er det til opplæring av operatører.*
- *Hva skal til for å bli selvstendig operatør*
- *Arbeidsbeskrivelse for operatører*

Vedlegg: Opplæringsplan for operatører

8.4 Tekniske modifikasjoner

- Tekniske modifikasjoner som kan gjøres av Operatør
Operatører kan kun skifte ødelagte deler, likt mot likt
- Tekniske modifikasjoner som må gjøres av *Teknisk personale:*
Store modifikasjoner skal kun utføres av labteknikere.

8.5 Personlig verneutstyr

Ved kontakt med oljen er vernebriller og hansker obligatorisk.

8.6 Generelt

- *Traverskran og truck kjøring skal ikke foregå i nærheten under eksperimentet.*
- *Vann og trykklufttilførsel i slanger skal stenges/kobles fra ved nærmeste fastpunkt når riggen ikke er i bruk.*

8.7 Sikkerhetsutrustning

8.8 Spesielle tiltak

9 TALLFESTING AV RESTRISIKO – RISIKOMATRISE

Se kapittel 13 "Veiledning til rapport mal.

Risikomatriksen vil gi en visualisering og en samlet oversikt over aktivitetens risikoforhold slik at ledelse og brukere får et mest mulig komplett bilde av risikoforhold.

IDnr	Aktivitet-hendelse	Frekv-Sans	Kons	RV
1	<i>Oljesøl: glatte gulv</i>	2	B	B2
2	<i>Kronglete område rundt riggen (Snubling)</i>	2	C	C2
3	<i>Øyeskader</i>	1	D	D1
4	Lang vei med trapp til manuell ventil for avstengning av luft	2	C	C2

Vurdering restrisiko: *Deltakerne foretar en helhetsvurdering for å avgjøre om gjenværende risiko ved aktiviteten/prosessen er akseptabel. Avsperring og kjøring utenom arbeidstid*

10 KONKLUSJON

Riggen er bygget til god laboratorium praksis (GLP).

Apparaturkortet får en gyldighet på **6 måneder**

Forsøk pågår kort får en gyldighet på **6 måneder**

11 LOVER FORSKRIFTER OG PÅLEGG SOM GJELDER

Se <http://www.arbeidstilsynet.no/regelverk/index.html>

- Lov om tilsyn med elektriske anlegg og elektrisk utstyr (1929)
- Arbeidsmiljøloven
- Forskrift om systematisk helse-, miljø- og sikkerhetsarbeid (HMS Internkontrollforskrift)
- Forskrift om sikkerhet ved arbeid og drift av elektriske anlegg (FSE 2006)
- Forskrift om elektriske forsyningsanlegg (FEF 2006)
- Forskrift om utstyr og sikkerhetssystem til bruk i eksplosjonsfarlig område NEK 420
- Forskrift om håndtering av brannfarlig, reaksjonsfarlig og trykksatt stoff samt utstyr og anlegg som benyttes ved håndteringen
- Forskrift om Håndtering av eksplosjonsfarlig stoff
- Forskrift om bruk av arbeidsutstyr.
- Forskrift om Arbeidsplasser og arbeidslokaler
- Forskrift om Bruk av personlig verneutstyr på arbeidsplassen
- Forskrift om Helse og sikkerhet i eksplosjonsfarlige atmosfærer
- Forskrift om Høytrykkspyling
- Forskrift om Maskiner
- Forskrift om Sikkerhetsskilting og signalgivning på arbeidsplassen
- Forskrift om Stillaser, stiger og arbeid på tak m.m.
- Forskrift om Sveising, termisk skjæring, termisk sprøyting, kullbuemeisling, lodding og sliping (varmt arbeid)
- Forskrift om Tekniske innretninger
- Forskrift om Tungt og ensformig arbeid
- Forskrift om Vern mot eksponering for kjemikalier på arbeidsplassen (Kjemikalieforskriften)
- Forskrift om Vern mot kunstig optisk stråling på arbeidsplassen
- Forskrift om Vern mot mekaniske vibrasjoner
- Forskrift om Vern mot støy på arbeidsplassen

Veiledninger fra arbeidstilsynet

se: <http://www.arbeidstilsynet.no/regelverk/veiledninger.html>

12 DOKUMENTASJON

- Tegninger, foto, beskrivelser av forsøksoppsetningen
 - Hazop_mal
 - Sertifikat for trykkpåkjent utstyr
 - Håndtering avfall i NTNU
 - Sikker bruk av LASERE, retningslinje
 - HAZOP_MAL_Procedyre
 - Forsøksprosedyre
 - Opplæringsplan for operatører
 - Skjema for sikker jobb analyse, (SJA)
 - Apparatorkortet
 - Forsøk pågår kort
-

13 VEILEDNING TIL RAPPORTMAL

Kap 7 Vurdering av teknisk sikkerhet

Sikre at design av apparatur er optimalisert i forhold til teknisk sikkerhet.

Identifisere risikoforhold knyttet til valgt design, og eventuelt å initiere re-design for å sikre at størst mulig andel av risiko elimineres gjennom teknisk sikkerhet.

Punktene skal beskrive hva forsøksoppsetningen faktisk er i stand til å tåle og aksept for utslipp.

7.1 Fareidentifikasjon, HAZOP

Forsøksoppsetningen deles inn i noder: (eks *Motorenhet, pumpeenhet, kjøleenhet.*)

Ved hjelp av ledeord identifiseres årsak, konsekvens og sikkerhetstiltak. Konkluderes det med at tiltak er nødvendig anbefales disse på bakgrunn av dette. Tiltakene lukkes når de er utført og Hazop slutføres.

(eks "No flow", årsak: rør er deformert, konsekvens: pumpe går varm, sikkerhetsforanstaltning: måling av flow med kobling opp mot nødstoppe eller hvis konsekvensen ikke er kritisk benyttes manuell overvåkning og punktet legges inn i den operasjonelle prosedyren.)

7.2 Brannfarlig, reaksjonsfarlig og trykksatt stoff.

I henhold til Forskrift om håndtering av brannfarlig, reaksjonsfarlig og trykksatt stoff samt utstyr og anlegg som benyttes ved håndteringen

Brannfarlig stoff: Fast, flytende eller gassformig stoff, stoffblanding, samt stoff som forekommer i kombinasjoner av slike tilstander, som i kraft av sitt flammepunkt, kontakt med andre stoffer, trykk, temperatur eller andre kjemiske egenskaper representerer en fare for brann.

Reaksjonsfarlig stoff: Fast, flytende, eller gassformig stoff, stoffblanding, samt stoff som forekommer i kombinasjoner av slike tilstander, som ved kontakt med vann, ved sitt trykk, temperatur eller andre kjemiske forhold, representerer en fare for farlig reaksjon, eksplosjon eller utslipp av farlig gass, damp, støv eller tåke.

Trykksatt stoff: Annet fast, flytende eller gassformig stoff eller stoffblanding enn brann- eller reaksjonsfarlig stoff, som er under trykk, og som derved kan representere en fare ved ukontrollert utslipp.

Nærmere kriterier for klassifisering av brannfarlig, reaksjonsfarlig og trykksatt stoff er fastsatt i vedlegg 1 i veiledningen til forskriften "Brannfarlig, reaksjonsfarlig og trykksatt stoff"

<http://www.dsb.no/Global/Publikasjoner/2009/Veiledning/Generell%20veiledning.pdf>

http://www.dsb.no/Global/Publikasjoner/2010/Tema/Temaveiledning_bruk_av_farlig_stoff_Del_1.pdf

Rigg og areal skal gjennomgås med hensyn på vurdering av Ex sone

- Sone 0: Alltid eksplosiv atmosfære, for eksempel inne i tanker med gass, brennbar væske.
- Sone 1: Primær sone, tidvis eksplosiv atmosfære for eksempel et fylle tappe punkt
- Sone 2: Sekundært utslippssted, kan få eksplosiv atmosfære ved uhell, for eksempel ved flenser, ventiler og koblingspunkt

7.4 Påvirkning av ytre miljø

Med forurensning forstås: tilførsel av fast stoff, væske eller gass til luft, vann eller i grunnen støy og rystelser påvirkning av temperaturen som er eller kan være til skade eller ulempe for miljøet.

Regelverk: <http://www.lovdatabasen.no/all/hl-19810313-006.html#6>

NTNU retningslinjer for avfall se: <http://www.ntnu.no/hms/retningslinjer/HMSR18B.pdf>

7.5 Stråling

Stråling defineres som

Ioniserende stråling: Elektromagnetisk stråling (i strålevernsammenheng med bølgelengde <100 nm) eller hurtige atomære partikler (f.eks alfa- og beta-partikler) som har evne til å ionisere atomer eller molekyler
--

Ikke-ioniserende stråling: Elektromagnetisk stråling (bølgelengde >100 nm), og ultralyd ¹ , som har liten eller ingen evne til å ionisere.
--

Strålekilder: Alle ioniserende og sterke ikke-ioniserende strålekilder.
--

Ioniserende strålekilder: Kilder som avgir ioniserende stråling, f.eks alle typer radioaktive kilder, røntgenapparater, elektronmikroskop
--

Sterke ikke-ioniserende strålekilder: Kilder som avgir sterk ikke-ioniserende stråling som kan skade helse og/eller ytre miljø, f.eks laser klasse 3B og 4, MR ₂ -systemer, UVC ₃ -kilder, kraftige IR-kilder ₄

¹ Ultralyd er akustisk stråling ("lyd") over det hørbare frekvensområdet (>20 kHz). I strålevernforskriften er ultralyd omtalt sammen med elektromagnetisk ikke-ioniserende stråling.
--

² MR (eg. NMR) - kjernemagnetisk resonans, metode som nyttes til å «avbilde» indre strukturer i ulike materialer.
--

³ UVC er elektromagnetisk stråling i bølgelengdeområdet 100-280 nm.
--

⁴ IR er elektromagnetisk stråling i bølgelengdeområdet 700 nm – 1 mm.
--

For hver laser skal det finnes en informasjonsperm(HMSRV3404B) som skal inneholde:

- Generell informasjon
- Navn på instrumentansvarlig og stedfortreder, og lokal strålevernskoordinator
- Sentrale data om apparaturen
- Instrumentspesifikk dokumentasjon
- Referanser til (evt kopier av) datablader, strålevernbestemmelser, o.l.
- Vurderinger av risikomomenter
- Instruks for brukere
- Instruks for praktisk bruk; oppstart, drift, avstenging, sikkerhetsforholdsregler, loggføring, avlåsning, evt. bruk av strålingsmåler, osv.
- Nødprosedyrer

Se ellers retningslinjen til NTNU for laser: <http://www.ntnu.no/hms/retningslinjer/HMSR34B.pdf>

7.6 Bruk og behandling av kjemikalier.

Her forstås kjemikalier som grunnstoff som kan utgjøre en fare for arbeidstakers sikkerhet og helse.

Se ellers: <http://www.lovdatabasen.no/cgi-wift/ldles?doc=/sf/sf/sf-20010430-0443.html>

Sikkerhetsdatablar skal være i forøkenes HMS perm og kjemikaliene registrert i Stoffkartoteket.

Kap 8 Vurdering av operasjonell sikkerhet

Sikrer at etablerte prosedyrer dekker alle identifiserte risikoforhold som må håndteres gjennom operasjonelle barrierer og at operatører og teknisk utførende har tilstrekkelig kompetanse.

8.1 Prosedyre Hazop

Prosedyre-HAZOP gjennomføres som en systematisk gjennomgang av den aktuelle prosedyren ved hjelp av fastlagt HAZOP-metodikk og definerte ledeord. Prosedyren brytes ned i enkeltstående arbeidsoperasjoner (noder) og analyseres ved hjelp av ledeordene for å avdekke mulige avvik, uklarheter eller kilder til mangelfull gjennomføring og feil.

8.2 Drifts og nødstop prosedyrer

Utarbeides for alle forsøksoppsetninger.

Driftsprosedyren skal stegvis beskrive gjennomføringen av et forsøk, inndelt i oppstart, under drift og avslutning. Prosedyren skal beskrive forutsetninger og tilstand for start, driftsparametere med hvor store avvik som tillates før forsøket avbrytes og hvilken tilstand riggen skal forlates.

Nødstopprosedyre beskriver hvordan en nødstop skal skje, (utført av uinnvidde), hva som skjer, (strøm/gass tilførsel) og hvilke hendelser som skal aktivere nødstop, (brannalarm, lekkasje).

Kap 9 Risikomatrise Tallfesting av restrisiko

For å synliggjøre samlet risiko, jevnfør skjema for risikovurdering, plottes hver enkelt aktivitets verdi for sannsynlighet og konsekvens inn i risikomatrisen. Bruk aktivitetens IDnr.

Eksempel: Hvis aktivitet med IDnr. 1 har fått en risikoverdi D3 (sannsynlighet 3 x konsekvens D) settes aktivitetens IDnr i risikomatrisesens felt for 3D. Slik settes alle aktivitetenes risikoverdier (IDnr) inn i risikomatrisen.

I risikomatrisen er ulike grader av risiko merket med rød, gul eller grønn. Når en aktivitets risiko havner på rød (= uakseptabel risiko), skal risikoreducerende tiltak gjennomføres. Ny vurdering gjennomføres etter at tiltak er iverksatt for å se om risikoverdien er kommet ned på akseptabelt nivå.

KONSEKVENNS	Svært alvorlig	E1	E2	E3	E4	E5
	Alvorlig	D1	D2	D3	D4	D5
	Moderat	C1	C2	C3	C4	C5
	Liten	B1	B2	B3	B4	B5
	Svært liten	A1	A2	A3	A4	A5
		Svært liten	Liten	Middels	Stor	Svært Stor
SANSYNLIGHET						

Prinsipp over akseptkriterium. Forklaring av fargene som er brukt i risikomatrisen.

Farge	Beskrivelse
Rød	Uakseptabel risiko. Tiltak skal gjennomføres for å redusere risikoen.
Gul	Vurderingsområde. Tiltak skal vurderes.
Grønn	Akseptabel risiko. Tiltak kan vurderes ut fra andre hensyn.

E Vedlegg til Risikovurderingsrapport

Vedlegg til Risikovurderingsrapport

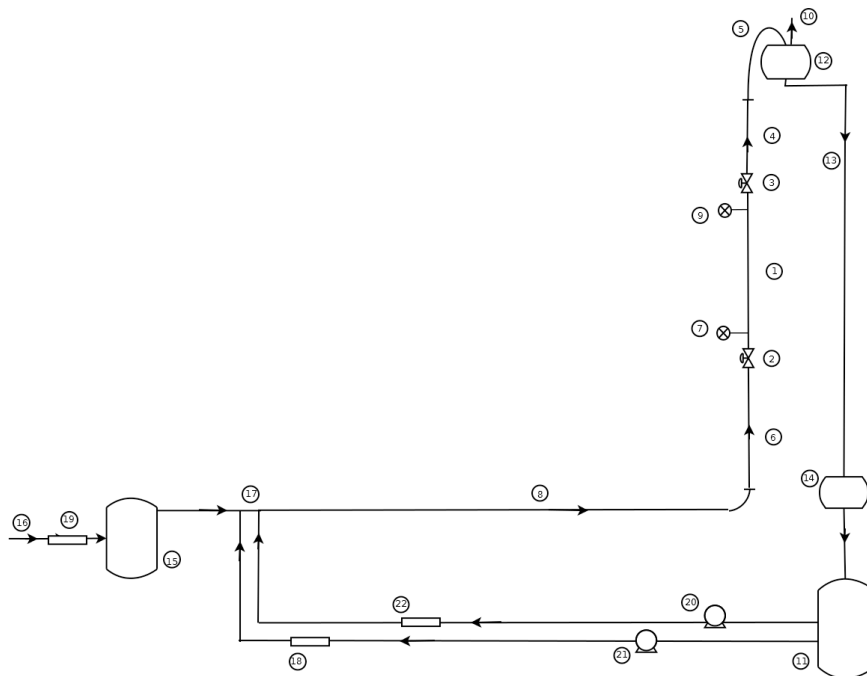
Gas Flow in Vertical Pipe with Wet Walls

Prosjekttittel	Experiments on gas flow with Wet Pipe Walls
Prosjektleder	Ole Jørgen Nydal
Enhet	NTNU
HMS-koordinator	Erik Langørgen
Linjeleder	OlavBolland
Plassering	VATL-FlerfaseLab
Romnummer	C164
Riggansvarlig	Andrea Shmueli, Thomas Arnulf

INNHALDSFORTEGNELSE

- VEDLEGG A PROSESS OG INSTRUMENTERINGSDIAGRAM (PID) 1
- VEDLEGG B HAZOP MAL..... 1
- VEDLEGG C FORSØKSPROSEDYRE 7
- VEDLEGG D OPPLÆRINGSPLAN FOR OPERATØRER..... 8
- VEDLEGG E APPARATURKORT UNITCARD 9
- VEDLEGG F FORSØK PÅGÅR KORT 10

• VEDLEGG A PROSESS OG INSTRUMENTERINGSDIAGRAM (PID)



ID	COMPONENT	ID	COMPONENT
1	STEEL TEST SECTION	12	OVERFLOW TANK
2	QUICK CLOSING VALVE	13	FLEXIBLE PIPE (DOWNFLOW SECTION)
3	QUICK CLOSING VALVE	14	SMALL SEPARATOR
4	ACRYLIC PIPE SECTION	15	BUFFER TANK (AIR)
5	FLEXIBLE PIPE (OUTLET)	16	INLET OF AIR FROM MAIN AIR SUPPLY
6	FLOW DEVELOPEMENT SECTION(STEEL)	17	INLET (ALL FLUIDS)
7	PRESSURE TRANSDUCER	18	MASS FLOW METER (WATER)
8	FLEXIBLE PIPE (HORISONTAL SECTION)	19	MASS FLOW METER (AIR)
9	PRESSURE TRANSDUCER	20	CENTRIFUGAL PUMP (OIL)
10	AIR OUTLET TO SURROUNDINGS	21	CENTRIFUGAL PUMP (WATER)
11	LARGE SEPARATOR	22	MASS FLOW METER (OIL)

• VEDLEGG B HAZOP MAL

Project: Gas Flow in Vertical Pipe with wet walls							Page
Node: 1 Oil and Water system							
Ref#	Guideword	Causes	Consequences	Safeguards	Recommendations	Action	Date/Sign
1	No flow	Pump not working. Operating at low pump frequency. Closed flowline valves	None	Physical inspection of the loop. Follow the startup procedure scheme in the lab	Stop pump	Check for any pump damage. Check if all the valves are opened. Check tank level.	
2	Reverse flow	Low air flow rate compared to fluid flow rate.	Fluids fill the buffer tank.	Increase the air flow rate before fluid flow rate. Control the buffer tank.	Stop pump and close the air valve.	Empty the buffer tank.	
3	More flow	High pump frequency	Minor vibration of flow lines	Operate with frequency boundary of 25-40 Hz	Lower the pump frequency.		
4	Less flow	Partial opening of the valves. Low pump frequency	Overloading of the pumps due to partial opening	Operate with frequency boundary of 25 – 40 Hz	Increase the pump frequency. Check flowline valves		
5	More level	No air, loop filled with liquid	None				
6	Less level	Inlet to pump closed	Dry-running of pumps				
7	More pressure	Valves not opened	Release of safety valve	Safety valve. Check valves in the procedure scheme			
8	Less pressure	See 1					

Project: Gas Flow in Vertical Pipe with wet walls							Page
Node: 1 Oil and Water system							
Ref#	Guideword	Causes	Consequences	Safeguards	Recommendations	Action	Date/Sign
9	More temperature	NA					
10	Less temperature	NA					
11	More viscosity	NA					
12	Less viscosity	NA					
13	Composition Change	NA					
14	Contamination	NA					
15	Relief	High air pressure from air system	Discharge to the atmosphere	Safety valves			
16	Instrumentation	Dirt, damage to sensors, wrong signal	No control of the system	Ensure the sensors are working well		System will always be visually monitored	
17	Sampling	NA					
18	Corrosion/erosion	NA					
19	Service failure	NA					
20	Abnormal operation	NA					
21	Maintenance	NA					
22	Ignition	NA					
23	Spare equipment	NA					
24	Safety	Water/Oil spill	Slippery floor	Physical inspection			

Project: Gas Flow in Vertical Pipe with wet walls							Page
Node: 2 Air system							
Ref#	Guideword	Causes	Consequences	Safeguards	Recommendations	Action	Date/Sign
1	No flow	Closed flow line valves. No air supply	Ref: reverse flow Node 1	Ensure that all valves in the flow line are open, ref: start-up procedure scheme	Stop liquid pump	Empty the buffer tank. Check that all valves are opened.	
2	Reverse flow	Air in oil/water loop	None				
3	More flow	Ref: More pressure Node 1					
4	Less flow	Partial opening of the valves.	Ref: reverse flow Node 1				
5	More level	NA					
6	Less level	NA					
7	More pressure	Sudden opening of the air valve. Error in the pressure regulator	Release of safety valve at 1.5 bar	Check pressure regulator		Close the air valve	
8	Less pressure	See 4					
9	More temperature	NA					
10	Less temperature	NA					
11	More viscosity	NA					
12	Less viscosity	NA					
13	Composition Change	NA					

Project: Gas Flow in Vertical Pipe with wet walls							Page
Node: 2 Air system							
Ref#	Guideword	Causes	Consequences	Safeguards	Recommendations	Action	Date/Sign
14	Contamination	NA					
15	Relief	High air pressure from air system	Discharge to the atmosphere	Safety valves			
16	Instrumentation	Dirt, damage to sensors, wrong signal	No control of the system	Ensure the sensors are working well		System will always be visually monitored	
17	Sampling	NA					
18	Corrosion/erosion	NA					
19	Service failure	NA					
20	Abnormal operation	NA					
21	Maintenance	NA					
22	Ignition	NA					
23	Spare equipment	NA					
24	Safety	Increase of air flow	Noise				

Project: Gas Flow in Vertical Pipe with wet walls							Page
Node: 2 Vertical riser system							
Ref#	Guideword	Causes	Consequences	Safeguards	Recommendations	Action	Date/Sign
1	No flow	Ref: Node 1 and 2	None				
2	Reverse flow	Ref: Node 1 and 2	Ref: Node 1 and 2				
3	More flow	High flow rates of fluids	Vibrations in pipes			Shut of pump, close air valve	
4	Less flow	See 2	Ref: reverse flow Node 1				
5	More level	See 3					
6	Less level	NA					
7	More pressure	Sudden opening of the air valve. Error in the pressure regulator	Release of safety valve at 1.5 bar	Check pressure regulator		Close the air valve	
8	Less pressure	See 4					
9	More temperature	NA					
10	Less temperature	NA					
11	More viscosity	NA					
12	Less viscosity	NA					
13	Composition Change	NA					
14	Contamination	NA					
15	Relief	Leakage	Discharge to the atmosphere	Safety valves			
16	Instrumentation	NA					

Project: Gas Flow in Vertical Pipe with wet walls							Page
Node: 2 Vertical riser system							
Ref#	Guideword	Causes	Consequences	Safeguards	Recommendations	Action	Date/Sign
17	Sampling	NA					
18	Corrosion/erosion	NA					
19	Service failure	NA					
20	Abnormal operation	NA					
21	Maintenance	NA					
22	Ignition	NA					
23	Spare equipment	NA					
24	Safety						

• **VEDLEGG C FORSØKSPROSEDYRE**

Experiment, name, number: Experiments on Gas Flow with Wet Pipe Walls	Date/ Sign
Project Leader: Ole Jørgen Nydal	
Experiment Leader: Andrea Shmueli	
Operator, Duties: Andrea Shmueli Thomas Arnulf	

	Conditions for the experiment:	Completed
	Experiments should be run in normal working hours, 08:00-16:00 during winter time and 08.00-15.00 during summer time. Experiments outside normal working hours shall be approved.	
	One person must always be present while running experiments, and should be approved as an experimental leader.	
	An early warning is given according to the lab rules, and accepted by authorized personnel.	
	Be sure that everyone taking part of the experiment is wearing the necessary protecting equipment and is aware of the shut down procedure and escape routes.	
	Preparations	Carried out
	Post the "Experiment in progress" sign.	
	<i>Follow and fill out startup-scheme for the multiphase flow rig</i>	
	During the experiment	
	<i>Start air supply</i>	
	Start liquid supply	
	Shut down liquid supply	
	Close quick closing valves and air supply	
	End of experiment	
	<i>Close valves for fluids (LabView)</i>	
	<i>Shut down pumps for fluids (LabView)</i>	
	Close air valve HV1001 manually	
	Remove all obstructions/barriers/signs around the experiment.	
	Tidy up and return all tools and equipment.	
	Tidy and cleanup work areas.	
	Return equipment and systems back to their normal operation settings	
	To reflect on before the next experiment and experience useful for others	
	Was the experiment completed as planned and on scheduled in professional terms?	
	Was the competence which was needed for security and completion of the experiment available to you?	
	Do you have any information/ knowledge from the experiment that you should document and share with fellow colleagues?	

• **VEDLEGG D OPPLÆRINGSPLAN FOR OPERATØRER**

Experiment, name, number: Experiments on Gas Flows With Wet Pipe Walls	
Project Leader: Ole Jørgen Nydal	Date/Sign
Operator Thomas Arnulf	

	Kjennskap til EPT LAB generelt	
	Lab - adgang - rutiner/regler - arbeidstid	
	Kjenner til evakueringsprosedyrer	
	Aktivitetskalender	
	Innmelding av forsøk til: iept-experiments@ivt.ntnu.no	
	Kjennskap til forsøkene	
	Prosedyrer for forsøk I flerfaselab	
	Nødstop	
	Nærmeste brann/førstehjelpsstasjon	
	Kjennskap til fluidene som benyttes I forsøket (Nexbase 3080)	
	Praktisk opplæring for kjøring av forsøket	

Jeg erklærer herved at jeg har gjennomgått og forstått HMS-regelverket, har fått hensiktsmessig opplæring for å kjøre dette eksperimentet og er klar over mitt personlige ansvar ved å arbeide i EPT laboratorier.

Operatør

Dato

Signert

- **VEDLEGG E APPARATURKORT UNITCARD**

Apparatur/unit

Dette kortet SKAL henges godt synlig på apparaturen! *This card MUST be posted on a visible place on the unit!*

Faglig Ansvarlig (Scientific Responsible) Ole Jørgen Nydal	Telefon mobil/privat (Phone no. mobile/private)
Apparaturansvarlig (Unit Responsible) Andrea Shmueli	Telefon mobil/privat (Phone no. mobile/private)
NTNU – Sintef Beredskapstelefon	800 80 388
Sikkerhetsrisikoer (Safety hazards) Olje med potensiell helserisiko benyttes	
Sikkerhetsregler Safety rules) Vernebriller og hansker skal benyttes ved håndtering av olje	
Nødstopprosedyrer Emergency shutdown) Pumpene skal slås av ved nødstoppsknappen. Ventil HV1001 skal stenges manuelt.	

Her finner du (Here you will find):

Prosedyrer (Procedures) ved kontrollbordet
Bruksanvisning (Users manual) ved kontrollbordet

Nærmeste (nearest)

Brannslukningsapparat (fire extinguisher)	Ved trappen, henger ved dør
Førstehjelpsskap (first aid cabinet)	Ved utgang til verksted

NTNU
Institutt for energi og prosessteknikk

Dato

Signert

- VEDLEGG F FORSØK PÅGÅR KORT

Forsøk pågår! Experiment in progress!

Dette kort skal settes opp før forsøk kan påbegynnes This card has to be posted before an experiment can start

Ansvarlig / Responsible Ole Jørgen Nydal	Telefon jobb/mobil/hjemme 73550564/97715994
Operatører/Operators Thomas Arnulf Andrea Shmueli	Forsøksperiode/Experiment time(start – slutt)
Prosjektleders signatur	Prosjekt Experiments on Gas Flow With Wet Pipe Walls
NTNU – Sintef Beredskapstelefon	800 80 388
Kort beskrivelse av forsøket og relaterte farer Short description of the experiment and related hazards Studere gasstrømning med en væskefilm på rørveggen. Lekkasje av olje vil gi glatte gulv Olje (Nexbase 3080) med potensiell helserisiko	

NTNU
 Institutt for energi og prosessteknikk

Dato

Signert
